

1996

Quantification of Tidal Creek Network Patterns using Fractal Methods

David C. Fugate

College of William and Mary - Virginia Institute of Marine Science

Follow this and additional works at: <https://scholarworks.wm.edu/etd>



Part of the [Physical and Environmental Geography Commons](#)

Recommended Citation

Fugate, David C., "Quantification of Tidal Creek Network Patterns using Fractal Methods" (1996).
Dissertations, Theses, and Masters Projects. Paper 1539617716.
<https://dx.doi.org/doi:10.25773/v5-sxzd-2a42>

This Thesis is brought to you for free and open access by the Theses, Dissertations, & Master Projects at W&M ScholarWorks. It has been accepted for inclusion in Dissertations, Theses, and Masters Projects by an authorized administrator of W&M ScholarWorks. For more information, please contact scholarworks@wm.edu.

**QUANTIFICATION OF TIDAL CREEK NETWORK PATTERNS
USING FRACTAL METHODS**

A Thesis
Presented to
The Faculty of the School of Marine Science
The College of William and Mary in Virginia

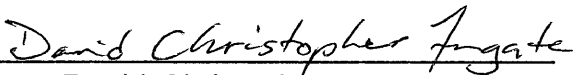
In Partial Fulfillment
Of the Requirements for the Degree of
Master of Arts

by
David C. Fugate
1996


APPROVAL SHEET

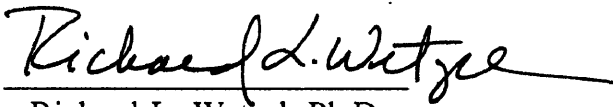
This thesis is submitted in partial fulfillment of
the requirements for the degree of

Master of Arts

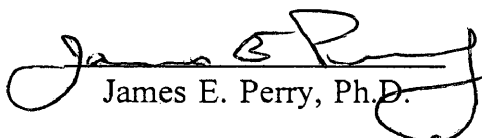

David Christopher Fugate

Approved, March 1996


David A. Evans, Ph.D.


Richard L. Wetzel, Ph.D.


Carl T. Friedrichs, Ph.D.


James E. Perry, Ph.D.

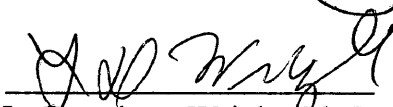

L. Donelson Wright, Ph.D.

TABLE OF CONTENTS

	Page
ACKNOWLEDGEMENTS	iv
LIST OF TABLES.....	v
LIST OF FIGURES.....	vi
ABSTRACT.....	vii
INTRODUCTION.....	2
FRACTAL DIMENSION AND ITS ESTIMATION.....	4
BACKGROUND.....	15
Morphodynamic Aspects.....	15
Energy Expenditure in creeks.....	20
Riverine vs. Tidal Creek Hydrology and Evolution.....	22
Morphodynamics in Ecological Context.....	24
Summary.....	25
OBJECTIVES.....	26
METHODS.....	27
Marsh Description.....	27
Preparations of Photographs for Analysis.....	30
The Functional Box Counting Method.....	30
Link Analysis.....	38
Rotation and Origin Variation.....	38
Hyperbola Fitting of Richardson Plot.....	39
Hortonian Analysis.....	41
RESULTS.....	43
Channel Analysis.....	43
Link Analysis.....	47
Hyperbola Fitting of Richardson Plot.....	49
Rotation and Origin Variation.....	49
Hortonian Analysis.....	55
DISCUSSION.....	59
Box-counting Technique.....	59
Relationship between Link and Channel Analysis.....	61
Hypothesis Testing of Richardson Plots.....	62
CONCLUSIONS.....	68
IMPLICATIONS.....	69
LITERATURE CITED.....	70

ACKNOWLEDGMENTS

I would like to gratefully acknowledge the help and guidance of my advisor, Dr. David A. Evans. Also I would like to acknowledge and give many thanks to Berch Smithson and David Wilcox for extensive technical help with this project.

LIST OF TABLES

1. Fractal Dimensions from Richardson Plots, Channel Analysis	48
2. Hyperbola Parameter Estimates.....	53
3. Hyperbola Parameter Estimates for Rotations of Wachapreague Marsh.....	56
4. Hortonian Analysis of Wachapreague Marsh.....	57
5. Hortonian Analysis of Wachapreague Marsh by Watershed.....	58

LIST OF FIGURES

1. Von Koch Curve and Variations.....	5
2. Interpretation of Standard Integer Dimension Figures in Terms of Exact Self-similarity and Extension to Non-integer Dimensioned Fractals.....	7
3. Examples of Richardson Plots.....	9
4. Example of Richardson Plot with Two Self-similar Regions.....	11
5. Color Infrared Aerial View of a Marsh.....	16
6. Color Infrared Aerial View of a Marsh.....	17
7. Color Infrared Aerial View of a Marsh.....	18
8. Role of Tidal Network Spatial Pattern in Ecological Processes.....	19
9. Theoretical Drainage Patterns.....	21
10. Marsh Locations.....	28
11. Scanned Photograph of Mockhorn Island	31
12. Scanned Photograph of Big Creek Marsh.....	32
13. Scanned Photograph of Wachapreague Marsh.....	33
14. Mockhorn Island Marsh Drainage Network.....	34
15. Big Creek Marsh Drainage Network.....	35
16. Wachapreague Marsh Drainage Network.....	36
17. Watershed Divisions of Wachapreague Marsh Network.....	42
18. Richardson Plots from Channel Analysis.....	44
19. Tangents to Richardson Plots from Channel Analysis.....	45
20. Tangents to Richardson Plots from Euclidean Analysis and Wachapreague Network.....	46
21. Wachapreague Marsh Linkage Pattern.....	50
22. Richardson Plots from Link Analysis.....	51
23. Tangents to Richardson Plots from Link Analysis.....	52
24. Observed and Predicted Richardson Plot from Mockhorn Island Network.....	54
25. Tangents to Richardson Plots from Channel and Link Analysis of Wachapreague Network.....	63
26. Tangents, Link vs. Channel Analysis, Mockhorn Island.....	64
27. Tangents, Link vs. Channel Analysis, Big Creek.....	65
28. Tangents, Link vs. Channel Analysis, Wachapreague.....	66

ABSTRACT

Whether a tidal creek erodes, accretes, or migrates depends on the biota, flow regime, and suspended sediment load, which are all related to and dependent upon the spatial pattern of the network through which the water flows. The topology of self similar patterns such as that exhibited by drainage networks may be quantified by their fractal dimension, a measure which does not suffer from scale dependencies as do traditional sinuosity measures. The degree of meandering in transgressing salt marsh drainage networks is empirically estimated as a fractal dimension using the functional box-counting technique. Variations of this technique are compared with each other, as well as with theoretically derived estimates of the fractal dimension. While establishing the fractal nature of the patterns, the Box-counting technique does not adequately determine the exact fractal dimensions of the patterns. An alternate method of quantifying the fractal behavior is employed by fitting the values derived from the Richardson plots to a hyperbolic curve.

QUANTIFICATION OF TIDAL CREEK NETWORK PATTERNS
USING FRACTAL METHODS

INTRODUCTION

Since Mandelbrot's innovative speculation on the fractal nature of stream networks there has been a fair amount of work to confirm and refine his ideas and predictions. Forms can be described as having a fractal structure if they are self similar over a range of scales of resolution, and exhibit increasing detail of form with increasing resolution (Mandelbrot, 1982, Tarboton, 1988, La Barbera, 1989). Many patterns in nature have been found to exhibit fractal behavior, such as cloud densities, carbon black particles, and landscape characteristics such as soil type, vegetation type, and river networks. Tidal channel networks, which may be highly branched and sinuous, provide an example of a pattern which is self similar with changing resolution. If one could take a photograph of a tidal network and enlarge a section of it, one would still see a branched and sinuous pattern. Likewise, an enlargement of this section would reveal more detail of the network, which would also be branched and sinuous. Fractal geometry allows the quantification of self similar patterns which previously had to be described in qualitative terms such as tortuous, grainy, or dendritic (Mandelbrot, 1982). The degree to which a tidal channel network is branched and sinuous may be measured by its fractal dimension. Fractal geometry also provides a method to realistically model natural systems.

I propose that the morphodynamic feedback processes of the marsh drainage network pattern, in concert with the laws of minimum energy dissipation, create a self organized process, whose telltale fractal insignia can be used to quantitatively compare critical states of

individual marsh systems. A thorough investigation of this idea is not within the scope of this work, instead as a beginning, some basic groundwork has been laid. Tidal channel networks seem intuitively to be fractal in nature. This project rigorously establishes the fractal nature of tidal channel networks, and produces quantitative estimates of their fractal dimension. The methodology of the "box-counting" technique is employed and investigated, and a new variation is applied.

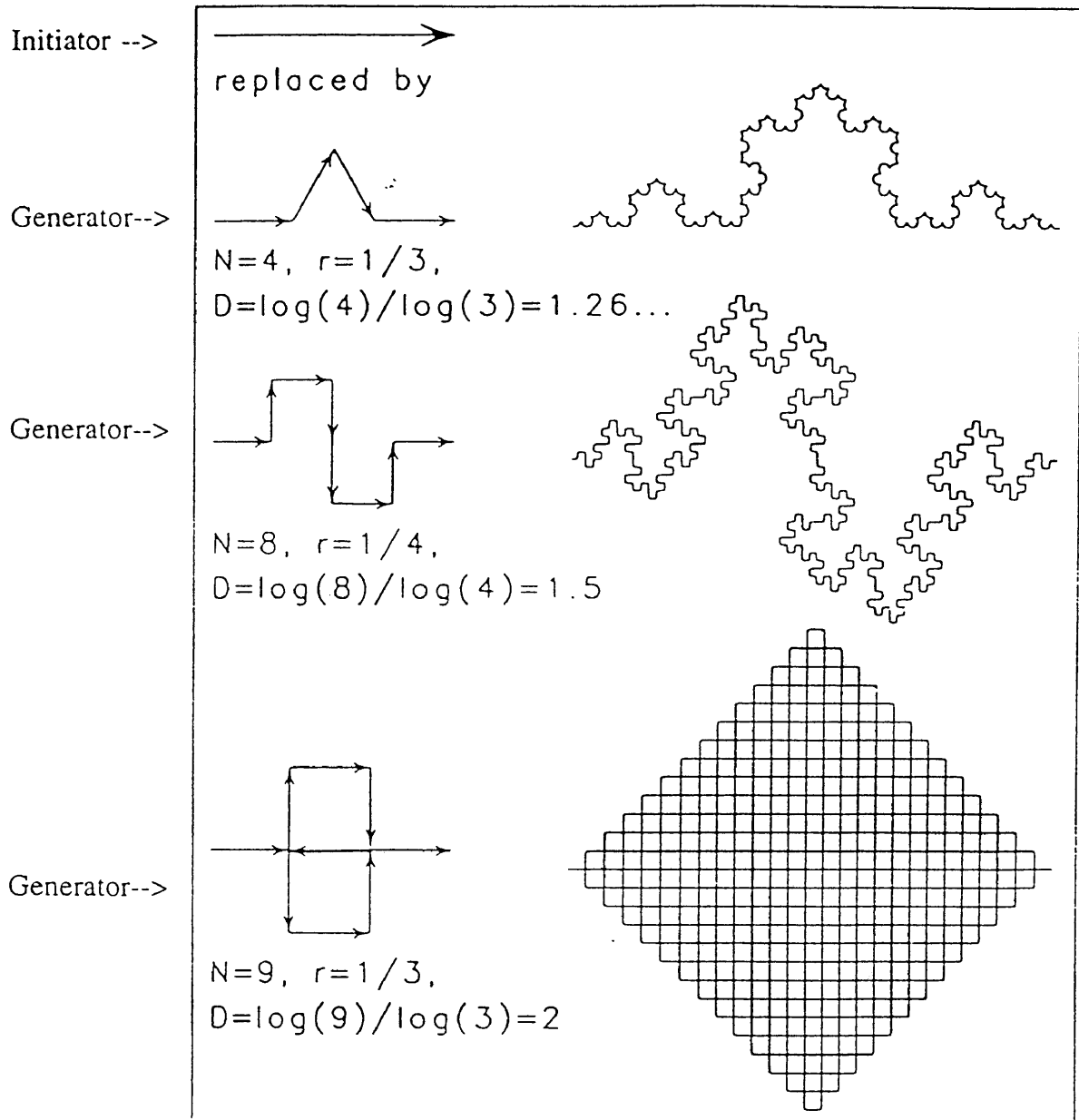
FRACTAL DIMENSION AND ITS ESTIMATION

The formal definition of a fractal object, according to Mandelbrot (1982), is a set for which the Hausdorff Besicovitch dimension strictly exceeds the topological dimension. For purposes of this project, a fractal object is one which exhibits increasing detail of form with increasing resolution, and which also is self similar across a range of resolutions (Mandelbrot, 1982, Tarboton, 1988, La Barbera, 1989).

An example of an ideal fractal curve is the von Koch snowflake, invented around 1904 (Figure 1). The curve is constructed through an iterative procedure in which each segment of the curve, called the initiator, is replaced with a pattern of segments, the generator. Each segment of the new curve is then replaced with the generator, and this process may continue infinitely. The generator consists of $N=4$ segments and the length of each segment is modified by a scaling factor of $r=1/3$ of the length of the initiator segment, so each iteration increases the length of the entire curve by $4/3$. Other examples are given in Figure 1. The von Koch curve is exactly self similar since increasing levels of magnification produce patterns which are identical.

The self similarity of a fractal pattern allows one to predict the degree of change in a topological measure of interest, e.g. length, from the amount of change of scale. This relation can be quantified by the fractal dimension of the object. Consider a straight line segment, which has an integer, or Euclidean dimension of 1. If the line is partitioned into $N=4$ equal

Figure 1. Von Koch Curve and Variations



(From Voss, 1988)

size segments, then each segment is scaled by $r=1/(N^{1/D})$ or $1/4$ (Figure 2). Similarly, a square on a two dimensional plane may be divided into $N=4$ similar squares. Each square is scaled by $r=1/(N^{1/2})$, or $1/2$. It can be seen that for any euclidean dimension D , an object with N similar parts, scaled down by a ratio of r gives:

$$N * r^D = 1$$

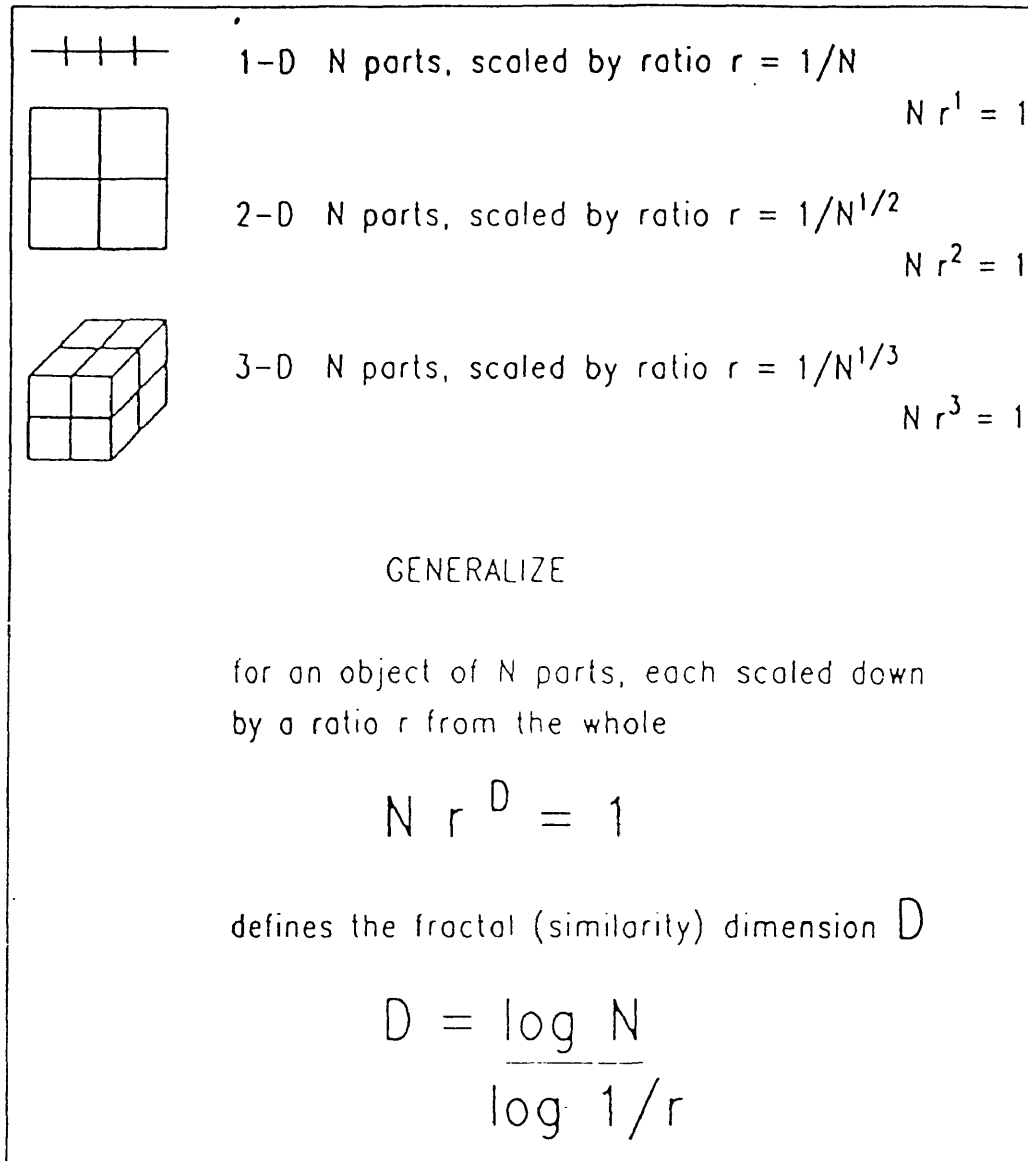
and so for any object of N self similar parts, scaled by a ratio of r from the whole, the fractal or similarity dimension is:

$$D = \frac{\log(N)}{\log(1/r)}$$

Remembering that for the von Koch snowflake, each generator consists of $N=4$ similar parts, each scaled $r=1/3$ from the next higher level, the fractal dimension = $\log(4)/\log(3)$, about 1.26. This non-Euclidean dimension between one and two describes the degree to which the curve fills up the space of the two dimensional plane. The fractal dimension can be used to characterize higher dimension objects, for example topography over a plane, with fractal dimension between 2 and 3, or xyz coordinates over time, with fractal dimension between 3 and 4.

Many natural patterns and processes exhibit fractal characteristics over a range of resolutions. These natural patterns, such as a coastline or stream pattern, expressing increasing detail and self similarity at different resolutions are considered nonideal or stochastic fractals. Richardson (1961) examined the relationship between the measured length of a coastline and the scales of the unit measure used to calculate it. The smaller the length

Figure 2. Interpretation of Standard Integer Dimension Figures in Terms of Exact Self-similarity and Extension to Non-integer Dimensioned Fractals



(From Voss, 1988)

of the unit measure, the longer is the total measured coastline length, since smaller 'rulers' capture smaller undulations of the coastline. If the coastline is very sinuous, then decreasing lengths of unit measure increase the total measured length of the coastline relatively more than would the same change in unit length for a straighter, smoother coastline.

If a coastline is measured with ruler length 'r', then:

$$length = r * N(r)$$

where $N(r)$ is the number of steps required to traverse the coastline. As with the ideal fractal of the von Koch snowflake, the number of steps required varies with the scaling factor $1/r^D$ so:

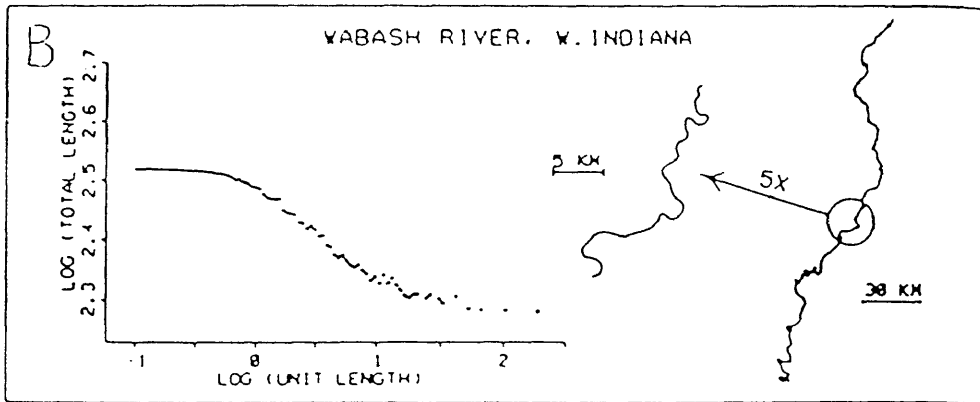
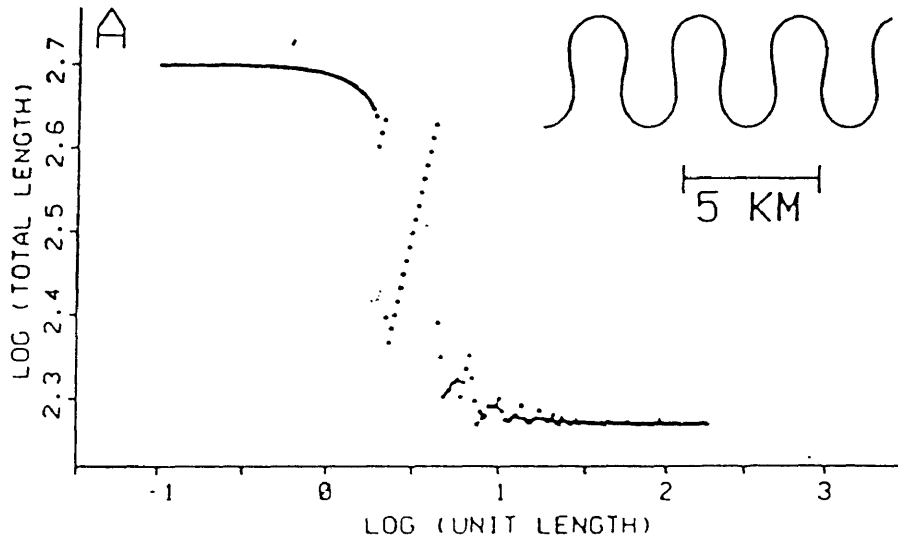
$$length \propto r * \frac{1}{r^D} \text{ or } \frac{1}{r^{(D-1)}}$$

The value of D for coastlines and river lengths can be empirically estimated by the use of Richardson plots.

A Richardson plot is constructed by plotting the log of the measured lengths by the log of the units of measure. If the pattern is fractal, then a straight line results over a significant part of the plot. The slope of this line is a measure of the sinuosity of the coastline and describes how the measure of coastline length changes with a change of scale. Mandelbrot incorporated Richardson's work and used the slope of this line to calculate the fractal dimension. Since then, Richardson plots have been used extensively to empirically derive the fractal dimension of natural patterns.

Figure 3 displays Richardson plots of simulated ideal stream meanders and single

Figure 3. Examples of Richardson Plots



Richardson plot of A: ideal meander and B: the Wabash R. (Snow, 1989)

threaded river lengths from Snow (1989). The first plot of an ideal meander, which is not fractal, shows three distinct regions, the two asymptotic regions to the right and left of the plot, and the broken area in the center of the plot. The more or less straight line area with a slope of zero to the left of the plot indicates the smoothness of the curve at very small scale. This region, typical for most Richardson plots, represents the range of the highest resolution of the curve or map from which the data was taken. The center disjointed region indicates the range over which periodicities occur in the ideal meanders, and the right region indicates the large scale ruler lengths over which no resolution of the meanders occur. The Wabash River, Indiana produces a more typical Richardson plot of a natural fractal object. The range over which the graph is a straight line with negative slope indicates the scale over which the pattern of the river exhibits fractal behavior. A similar region is clearly missing from the idealized meanders, which do not contain increasing detail with increasing resolution. A pattern may exhibit different levels of fractal behavior at different scales. (Nikora, 1991) This phenomenon is indicated when two or more straight line segments of the Richardson plot occur at different ranges (Figure 4).

River networks have long been characterized by bifurcation and length ratios, measures developed by Horton (1945) and Strahler (1952). Hortonian analyses assume that the bifurcation ratios and length ratios between stream orders are constant across all stream orders. The bifurcation ratio is:

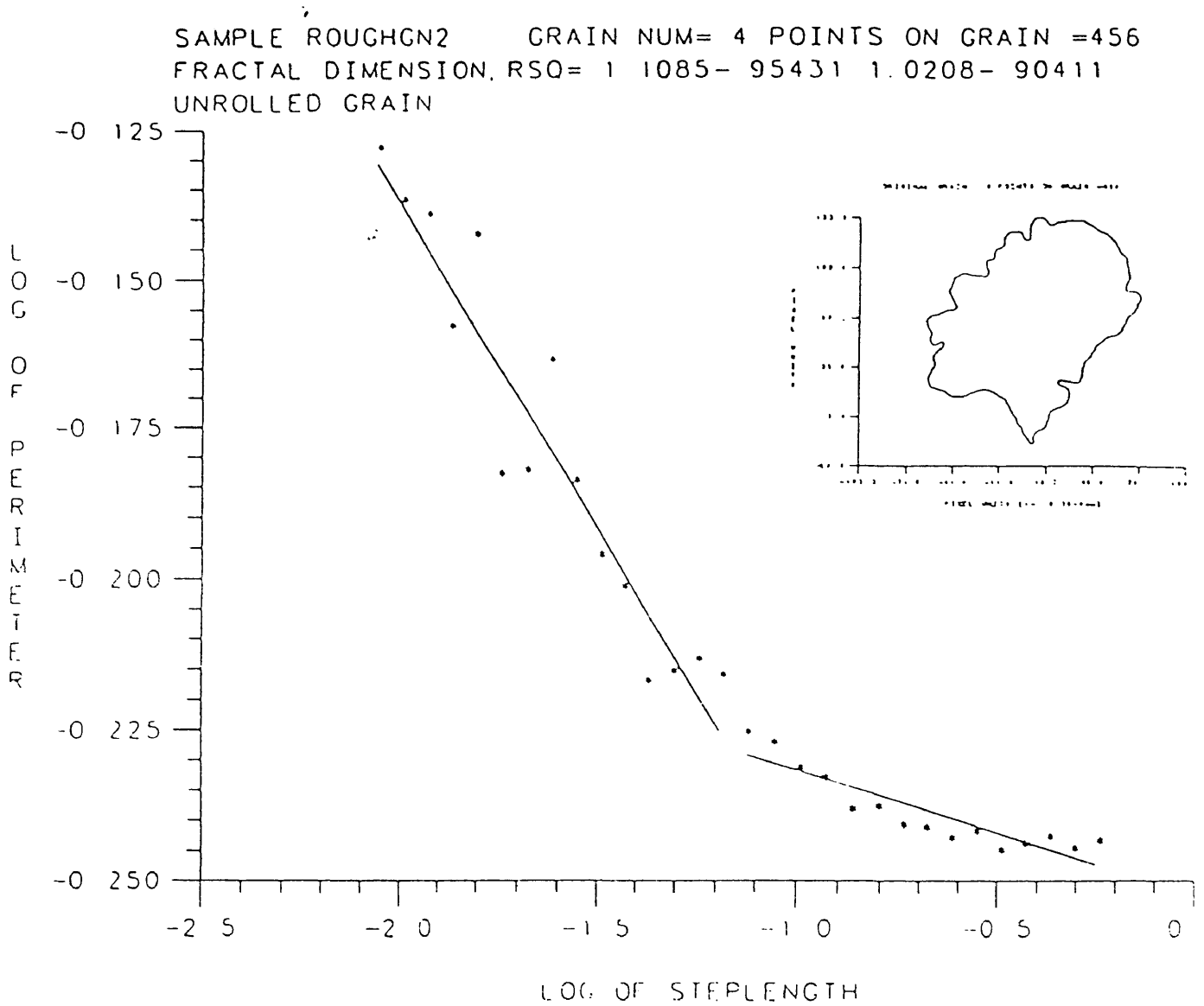
$$R_b = N_{w-1} / N_w$$

and the length ratio is:

$$R_l = L_w / L_{w-1}$$

where N_w is the number of streams of order w , and L_w is the mean length of stream or order

Figure 4. Example of Richardson Plots with Two Self-similar Regions



Richardson plot of a digitized rough particle showing two self-similar regions (Frisch, 1988)

w. These measures may be linked to two aspects of river networks which exhibit fractal behavior, the sinuosity of the streams (Mandelbrot, 1983, Hjelmfelt, 1988), and the degree of branching of the stream network (Tarboton, 1988, 1990, La Barbera and Rosso 1989, 1990). There is still discussion on the exact derivation of the fractal dimension from the bifurcation and length ratios, but their forms are similar. A summary, provided by Nikora (1993) follows:

La Barbera and Rosso [1987,1989]

$$D = \frac{\ln R_B}{\ln R_L}$$

Nikora [1988] and Nikora et al. [1989]

$$D = \frac{\ln R_B}{\ln R_L} = \frac{\ln R_B}{\ln R_p} = 2 \frac{\ln R_B}{\ln R_A}$$

Tarboton et al. [1988,1990]

$$D = d \frac{\ln R_B}{\ln R_L}$$

La Barbera and Rosso [1990]

$$D = \frac{1}{2 - d} \frac{\ln R_B}{\ln R_L}$$

and Rosso et al. [1991]

$$D = d \frac{\ln R_B}{\ln R_L} = 2 \frac{\ln R_B}{\ln R_A}$$

where D is fractal dimension, R_B is the bifurcation ratio, R_L is the length ratio, R_A is the catchment area ratio, R_p is the perimeter of the catchment area, and d is a constant.

Another method of determining the fractal dimension of patterns is the functional box-counting method. The pattern of interest is overlaid with grids of varying mesh size. If r is the length of a side of a cell, with area r^2 , and $N(r)$ is the number of cells which contain an element of the pattern, then (if the pattern follows fractal behavior):

$$N(r) \propto r^{-D}$$

and Richardson plots may be constructed to empirically determine D . The box-counting method can be extended using cubes of higher dimensions if desired (Barnesly, 1988, Mandelbrot, 1982).

Tidal channels do not have hierarchical orders of streams and tributaries as single channel river networks do, instead they more closely resemble braided river networks. This prevents characterization using Hortonian measures, which may, in any case, be labor intensive. For the same reason, they are not amenable to analysis using the 'ruler' method

which Richardson used on coastlines. Nikora (1991) has employed the functional box-counting method to determine the fractal dimension of braided rivers. The same methodology can be used to determine the fractal dimension of tidal networks.

When employing the box-counting method, the grid should overlay the pattern of interest so that the count of the number of boxes which cover the pattern is a minimum. (Barnesly 1988, Garcia-Ruiz, 1992). Voss (1988) suggests using the box-counting method by placing the grids over the pattern at many different origins and using the mean value obtained for the fractal dimension. This obviously requires significantly more time and effort, and careful reading of past research using the box-counting method suggests that it is rarely attempted. The results of the box-counting method may also be affected by the angle of rotation of the grid. Ragotzkie (1959) used a method similar to box-counting in which he overlaid parallel lines on a tidal network plan and counted the number of intersections of the patterns with the lines. He notes that this method may be sensitive to anisotropy in the network, but concludes that most networks lack directional orientation. This project explores the robustness of single sampling of grid origin and angle of rotation.

BACKGROUND

Morphodynamic Aspects

The hydrology and geometry of tidal creeks form a morphodynamic feedback system. The geometry of tidal creeks determines the hydrology, the hydrology determines the sediment transport, and the sediment transport, in turn, determines the geometry. The ecological processes of the marsh are intimately related to this system. The highly branched and sinuous creek system shown in Figure 5 will retard the transport of nutrients and sediment through frictional damping of the water flow more than a creek system with relatively straighter creeks such as the one in Fig 6. Another type of tidal creek network system is shown in Figure 7. The hydrology and consequently, the sediment and nutrient flux, of this system are affected by the ponding that is typical of drowning salt marshes such as this one.

The interaction of the ecological and physical processes in the boundary layer is an important component of the creek pattern morphodynamics. Bed forms and substrate erodibility are mediated by the biology through algal and bacterial mats, polychaetes, shellfish, and fiddler crabs. (Wildish and Miyares, 1990, Escartin and Aubrey, 1995). These organisms change the roughness and the critical shear stress of the bed, and affect the amount of energy which must be expended by the flow (Figure 8).

Figure 5. Color Infrared Aerial View of a Marsh



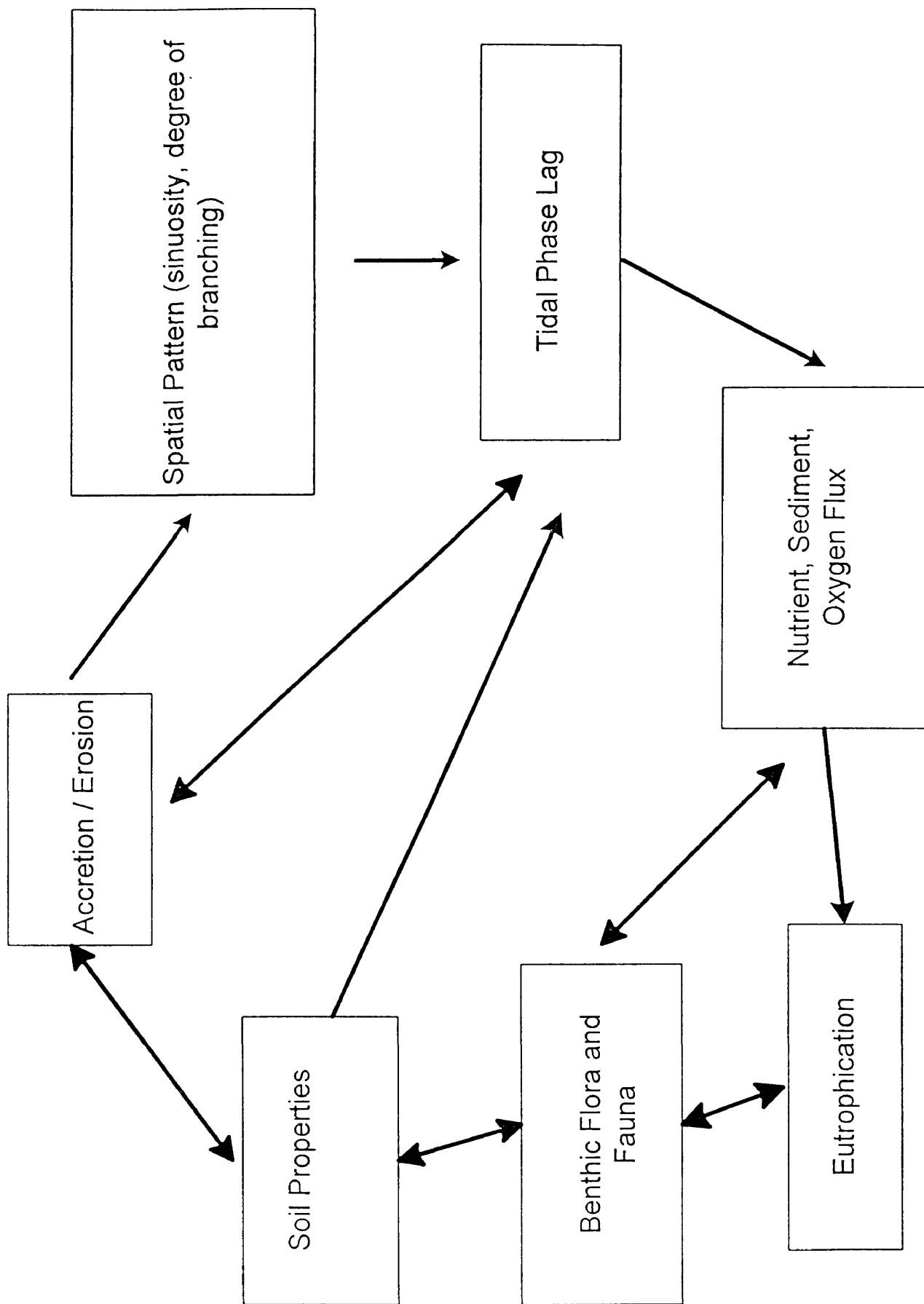
Figure 6. Color Infrared Aerial View of a Marsh



Figure 7. Color Infrared Aerial View of a Marsh



Figure 8. Role of Tidal Network Spatial Pattern on Ecological Process



Energy Expenditure in Creeks

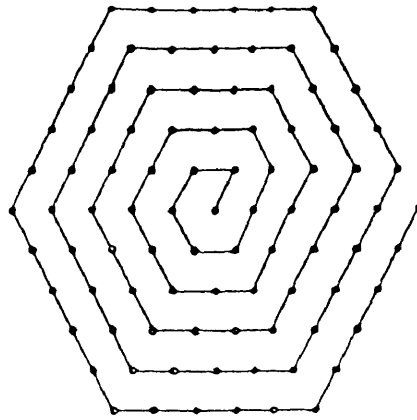
The typical dendritic pattern of riverine drainage systems has been shown to be related to the laws of minimum energy dissipation (eg. Rodriguez-Iturbe(1992)). These laws, posited by Leopold and Langbein (1962) are:

1. Minimum energy is expended in any link of a drainage network.
2. The energy expended per unit area is the same everywhere in the network.
3. The energy expenditure of the system as a whole is minimized.

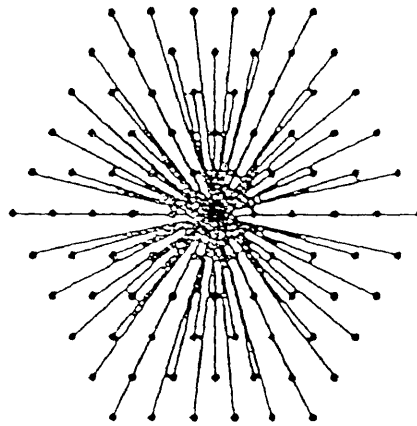
A quick illustration of how this branching can result from these laws can be found in Steven's 'Patterns in Nature' (1974) from which Figure 9 was derived. Consider each pattern as a drainage system with the outlet in the center. The dots are particles of water, and the amount of energy expended by the water can be related to the length of the path that the water follows. The energy expended by the system as a whole is proportional to the sum of the length of all the paths. The first pattern results in the minimum energy expended for the system as a whole, but the average energy expended by each individual particle is relatively large. The second pattern results in the minimum average energy expenditure for each individual particle, but has a high over all energy expenditure. The last, branched pattern, provides a balance between the first and the second pattern.

The fractal nature of riverine network patterns and their relation to the laws of minimum energy has been explored by Rodriguez-Iturbe (1992). He found that river network models simulated by application of these laws resulted in structures whose fractal nature was

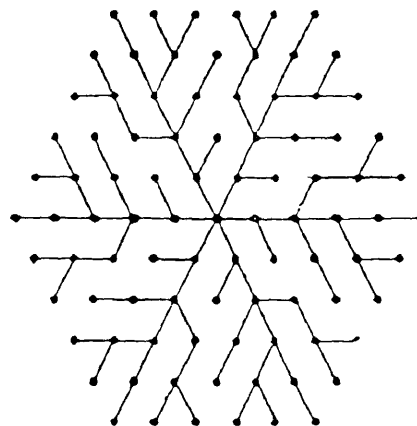
Figure 9. Theoretical Drainage Patterns



$$L_T = 90$$
$$\bar{L} = 45.5$$



$$L_T = 233.1,$$
$$\bar{L} = 3.37$$



$$L_T = 90$$
$$\bar{L} = 3.73$$

(From Rodriguez-Iturbe, 1992)

indistinguishable from that of natural river networks. Per Bak (1987) has suggested that fractal structures in space are indicators of self organizing critical processes. A natural system may maintain long term stability through small scale instability and episodic catastrophic events. In a tidal network system, bank slumping may be envisioned as the result of small scale instabilities, and storm and flooding events as catastrophic factors which shape the tidal network patterns. Though the actual channels may migrate, the sinuosity, branching characteristics, and channel density of the entire network maintain a stable state over time, as manifest by a temporally constant fractal dimension.

Riverine vs Tidal Creek Hydrology and Evolution

The flow through a tidal network is significantly different from flow through a river network. Not only is the flow bidirectional, but maximum flow, called bankfull discharge, occurs with regularity, in contrast to river systems which may experience bankfull discharge only during seasonal flood events. Most physical reworking in stream channels is considered to occur during bankfull discharge (Pestrong, 1965), and so we might expect the spatial pattern of tidal creeks to adjust relatively quickly to anthropogenic or other perturbations in the morphodynamic system, such as ditching and storm events. Tidal creeks might be expected to exhibit fractal behavior in response to the same principles which guide riverine dendritic pattern development, but to exhibit different values for their fractal dimension.

The initial development of tidal network systems is also different from that of a riverine drainage system. A transgressing estuarine marsh invades mature upland systems as it migrates landward with rising sea level. Creek geomorphology, hydrology, and community

structure along with associated processes such as nutrient and sediment flux follow a gradient from the ephemeral immature creeks at the landward edge to the mature stable creeks at the mouth. The shallow ephemeral creeks are filled for less than half of the tidal stage, hence they are flood dominated and tend to import nutrients and sediment (Boone and Byrne, 1981, Friedrichs and Aubrey, 1988). As the creek matures, the sinuous and unstable patterns of these ephemeral creeks become established by constraint of the lateral flow (Murray and Paola, 1994), presumably through vegetation colonization. With rising sea level the channels deepen and the tidal velocity asymmetry tends toward ebb dominance. The once ephemeral creeks must adjust to a geometrically increasing amount of discharge, as determined by the hypsometry of the marsh, and a concomitant amount of energy dissipation. This transition under the principles of equal and minimum energy dissipation begins to reshape the meanders formed under flood dominance and may account for the difference in sinuosity between old and new creeks. The transitional creeks have been found to have the highest sinuosity, followed by the ephemeral creeks, and least sinuous, the older mature creeks (Dame et al, 1992.) The changing flow regime changes the spatial distribution of the shear stresses experienced by the banks of the immature creeks, producing new bends and contours through erosion, thereby increasing the sinuosity. Eventually ebb erosional forces begin to straighten out the creek while dikes vegetated by tall-form *Spartina* form on the edge. The tall-form *Spartina*, initiated by the high flushing rate at the bank, create a positive feedback for increased growth by attracting *Uca*, who further increase flushing levels through bioirrigation. The straighter deeper mature creek with more durable banks tends to export nutrients and particulates.

Lagoonal and prograding marshes do not experience this changing discharge with

evolution. Instead, once a creek is formed, it always drains a constant amount of area, while the marsh extends lagoonward. If the degree of sinuosity and branching is a response to the amount of energy which must be dissipated, then the patterns of similarly aged creeks will differ between lagoonal and transgressing marsh systems.

Morphodynamics in Ecological Context

Water is the transport medium for suspended sediment, nutrients, and salinity in and out of a tidal marsh. The flow of water is directly determined by the creek geometry and friction along the bed and bank. At the same time, the flow may modify the geometry through deposition of suspended material or erosion of the bed or banks. The relatively flat slopes, shallow channels, and soft sediments make friction an important component in the flow of water through tidal networks. A high degree of sinuosity and branching creates more area for the flow to cross and amplifies the effect of these factors. The frictional damping of the tidal flow, as well as the increased distance between some parts of the marsh and open water may result in a feedback loop between the physical and biological processes within the network. As the tidal exchange efficiency is decreased, the nutrient flux in and out of the marsh is affected. A tidal network, or portion thereof, with a high fractal dimension might be expected to have a low tidal exchange efficiency, which would retard export or import of nutrients, and so play an important role in determining the biotic processes and community structure there. Results from studying import and export of nutrients from different tidal marshes vary widely (e.g. Jordan and Correll, 1991). Differences in fractal dimension may help explain differences in nutrient flux between marshes.

Summary

The energy expenditure of the water flow in the marsh is a function of the tidal prism, distortion of the tidal cycle, underlying geography, and all the biogenic processes affecting the soil. These processes and the feedbacks between them should be embodied in the network pattern. So we might expect marshes which have similar processes to exhibit, not the exact same pattern, but patterns which similarly dissipate the energy of the system, and thus to have the same fractal dimension. Marshes which are functionally different with respect to import or export of nutrients, or different evolutionally, or different in other factors may exhibit different fractal dimensions.

OBJECTIVES

To examine these ideas I have analyzed three marshes on the Eastern Shore, Virginia, relative to the following objectives:

1. Determine if tidal networks are spatially distributed in a fractal manner over a defined range of scales.
2. If so, determine the fractal dimension over these scales for tidal networks on the Eastern Shore, Va.
3. Compare and evaluate the consistency of the fractal dimension among the tidal networks.

In addition , the following tests of the functional box-counting methodology were performed:

4. Test the robustness of the box-counting technique to various rotations and origins of the overlaid grid.
5. Compare the results empirically derived from the box-counting technique with the results from applying the theoretically derived equations for the fractal dimension as a function of the bifurcation and length ratios.

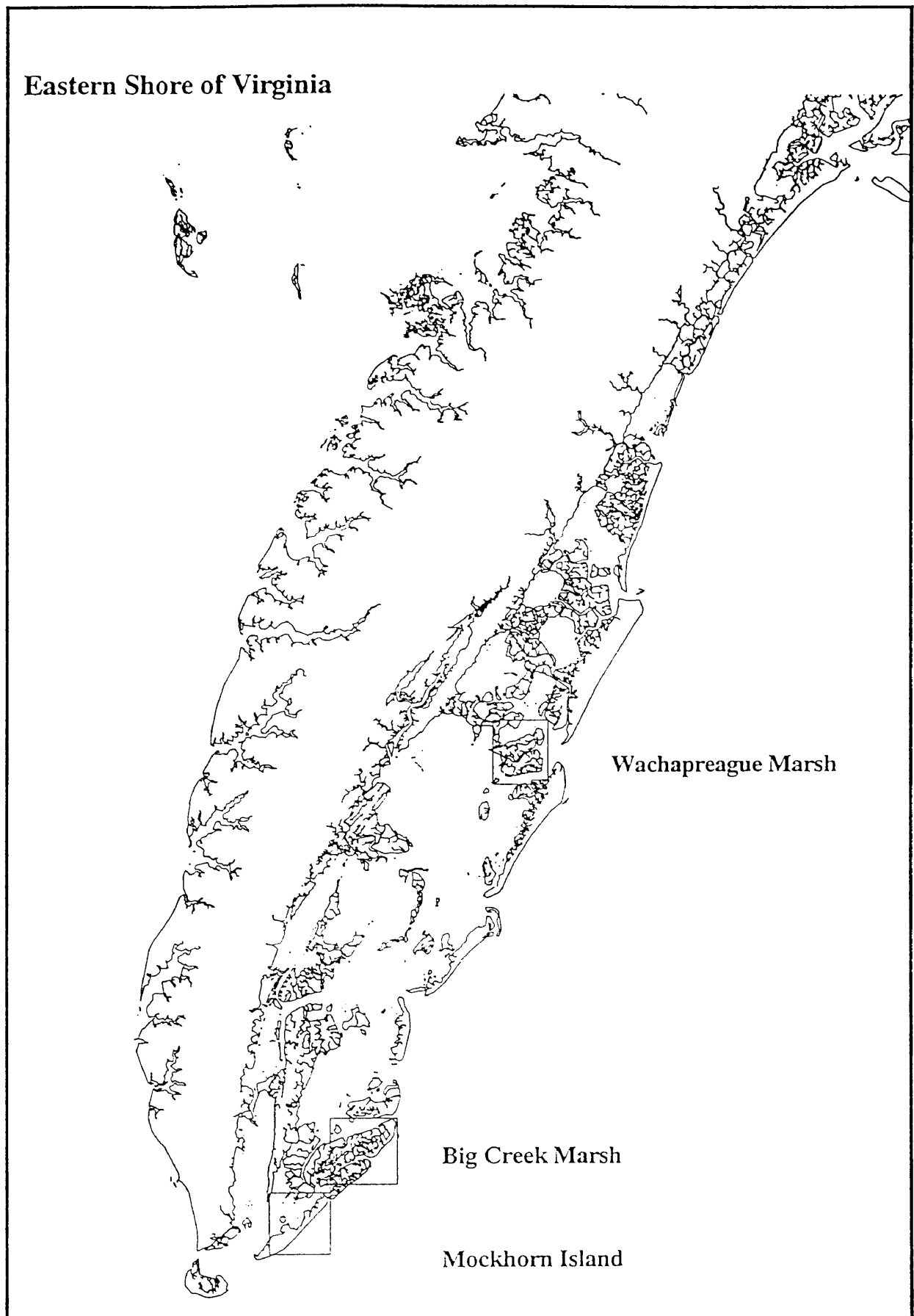
METHODS

Marsh Description

The three drainage network patterns analyzed are parts of large marsh expanses behind back barrier islands located on the Eastern Shore, Virginia (Figure 10). They are lagoonal marshes with well developed drainage patterns and creeks perhaps hundreds of years old (Osgood and Zieman, 1993), with no appreciable freshwater input. The vegetation is dominated by tall, medium, and short form *Spartina alterniflora*, and *Juncus roemerianus*. The tidal range is about 1.25 meters. Sea level rise has been estimated to be 2.8 - 4.22 mm/yr in the last 60 years (Oertel et al, 1989).

The final drainage network patterns cover areas of 2193 by 2176, 2986 by 7240, and 6150 by 10600 square meters for the Wachapreague, Big Creek, and Mockhorn Island marshes, respectively.

Figure 10. Marsh Locations



This page is intentionally left blank.

Preparation of Photographs for Analysis

Color infrared photographs were taken of the three marshes at an altitude of 5000 feet using nine inch format S2443 film with a T-11 areal camera, 152.4 mm lens, resulting in a field of view of 73 degrees. Two overlapping photographs of Wachapreague marsh and Big Creek marsh were used.

The photographs were scanned at a pixel width of 25 microns, about 1000 dpi, using a Vexcel scanner by ImageScans, Denver, Colorado. The scanned images (Figures 11-13) were then converted into an ERDAS format, and georeferenced to Universal Transverse Mercator coordinates against digitized shoreline coverages prepared by the Virginia Institute of Marine Science's Resource Management and Policy Department. The creek networks for each photograph were then digitized into an arc coverage using ARC-INFO software. The maximum error of this digitizing was 3 meters (the snap distance), but usually was no more than 1 meter. All creeks as narrow as 3 meters were digitized. The coverages of adjacent photographs were then joined using the Link and Edgematching facilities of ARC-INFO. The final drainage network patterns for the three marshes are shown in Figures 14-16, with resolutions around, for the Wachapreague marsh for example, 0.32 meters width per pixel. This is significantly higher resolution than is available through USGS digitized hydrology.

The Functional Box-counting Method

The functional box-counting method was performed as described by e.g. Lovejoy(1988) and Voss(1988)) upon the arc coverages of the three marshes. Using ARC-INFO software, each coverage was gridded at log increments. Preliminary analyses suggested

Figure 11. Scanned Photograph of Mockorn Island

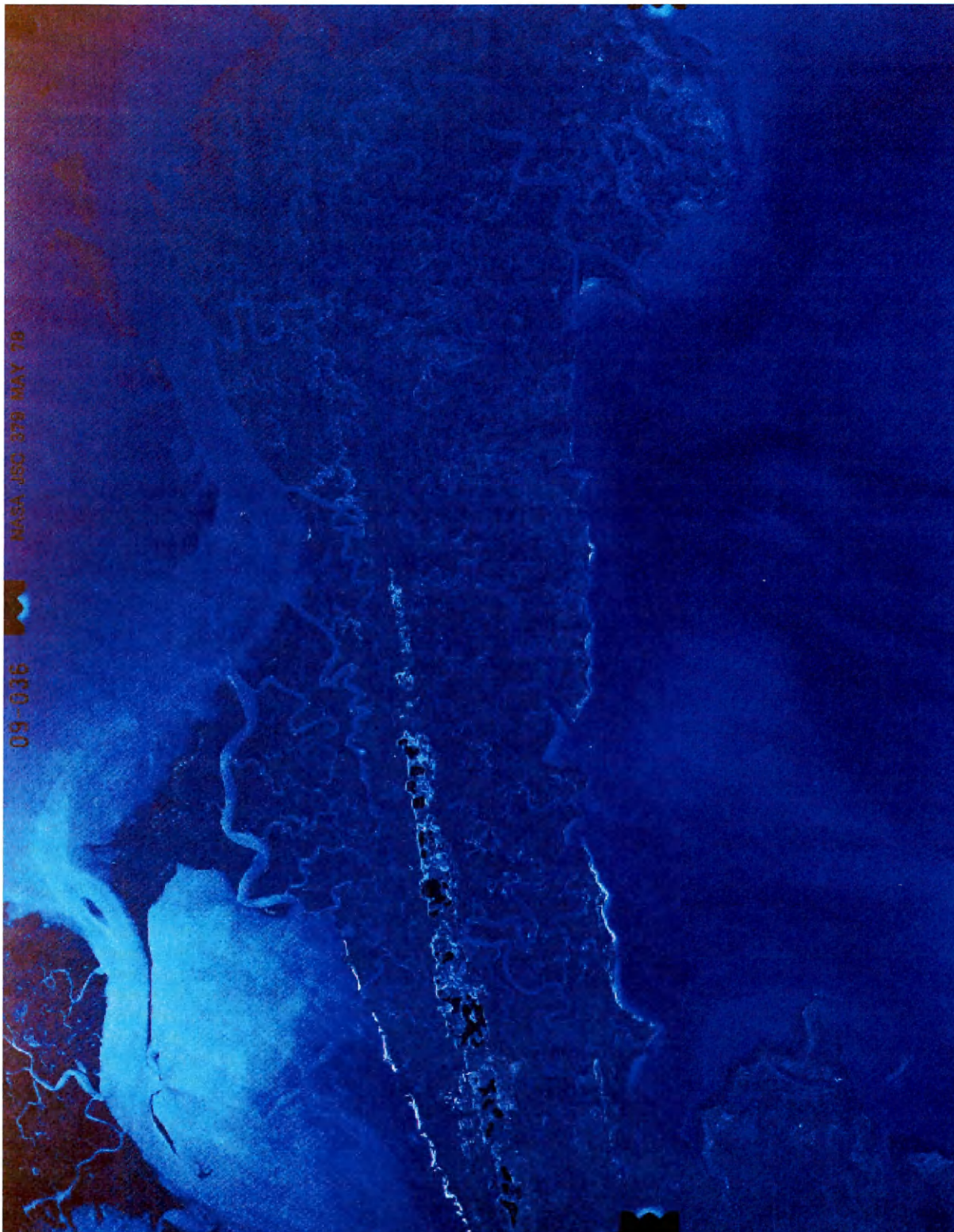


Figure 12

Scanned Photograph of Big Creek Marsh



Figure 13. Scanned Photograph of Wachapreague Marsh

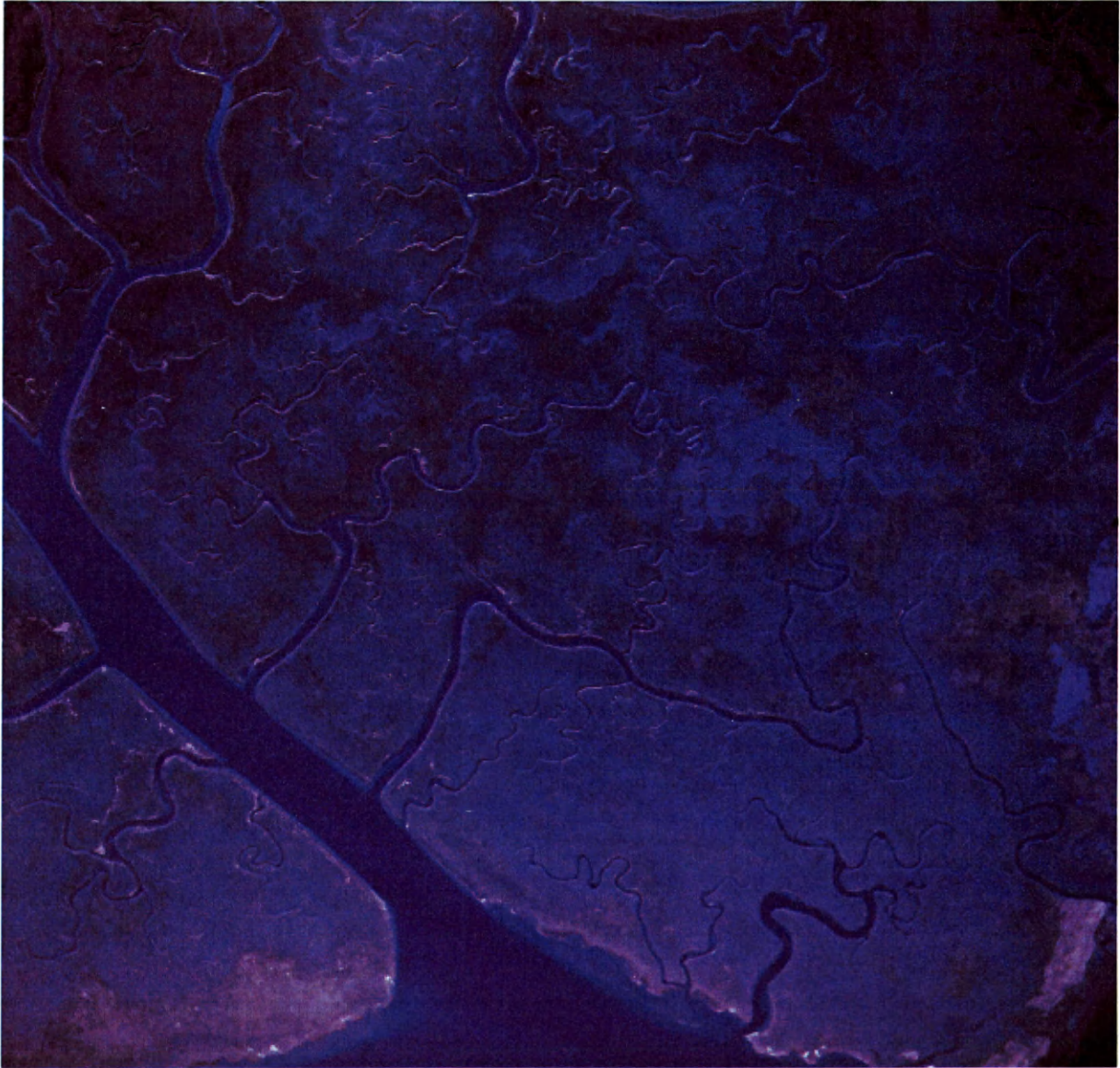


Figure 14

Mockhorn Island Marsh Drainage Network

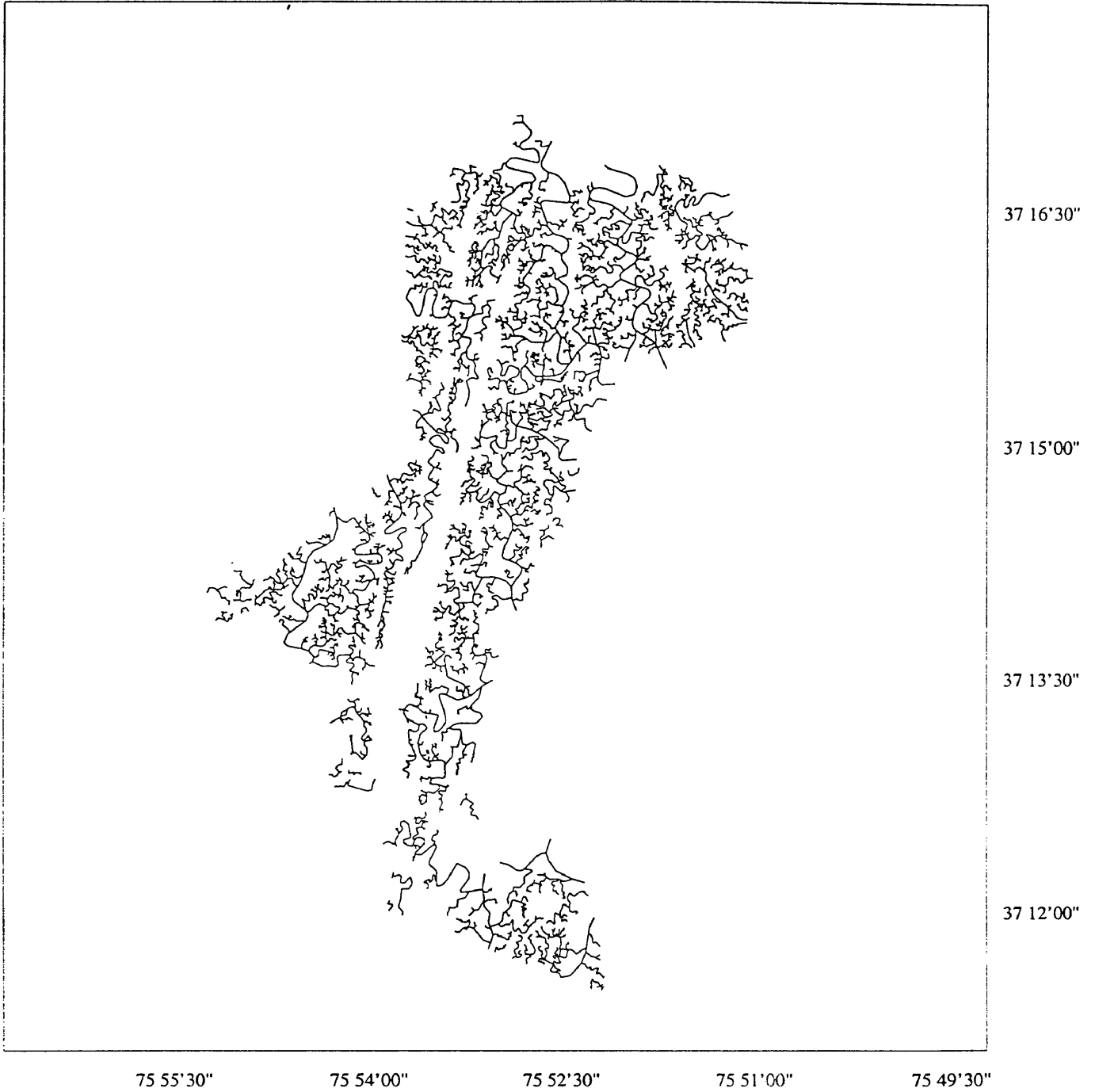


Figure 15

Big Creek Marsh Drainage Network

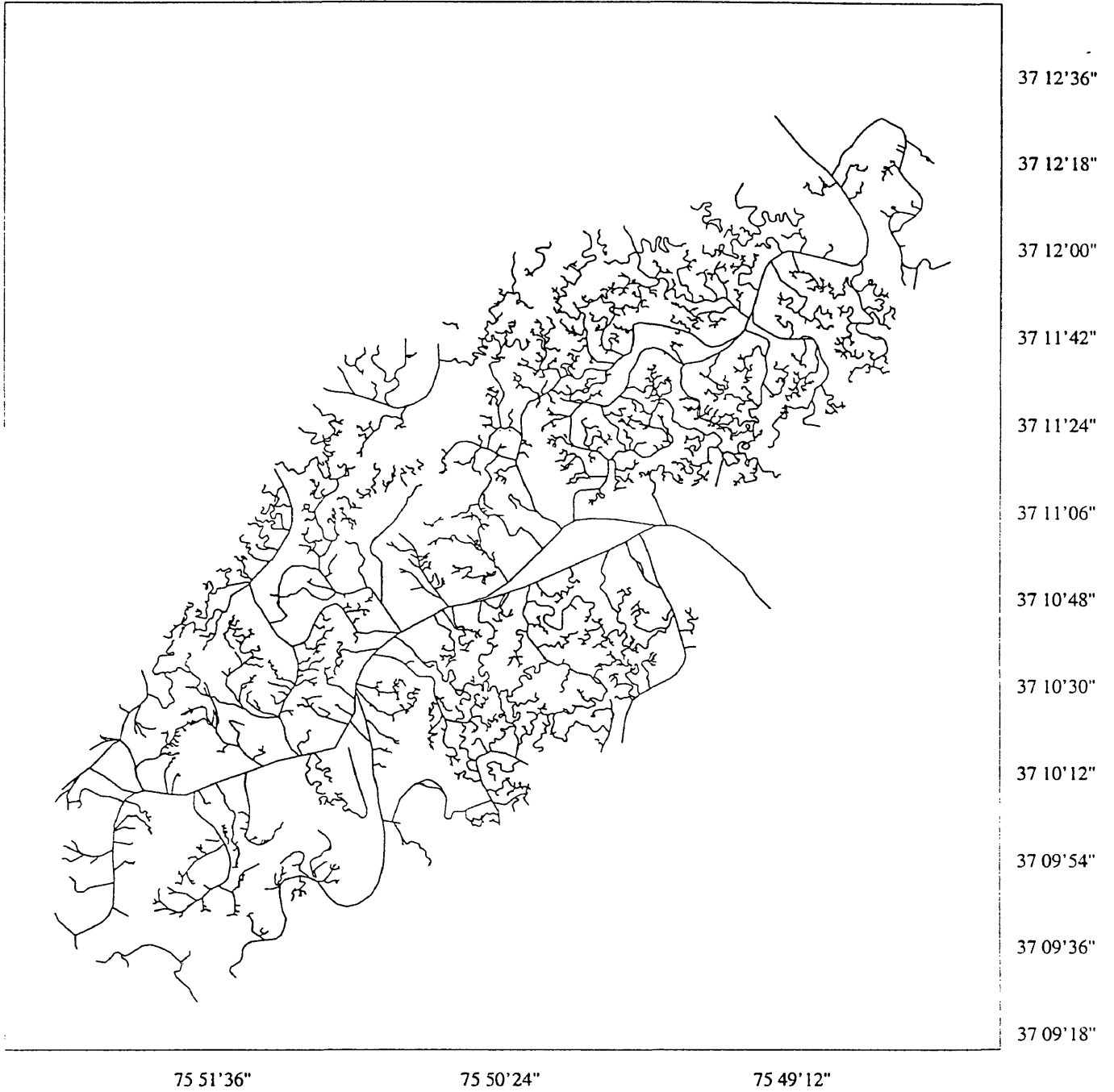
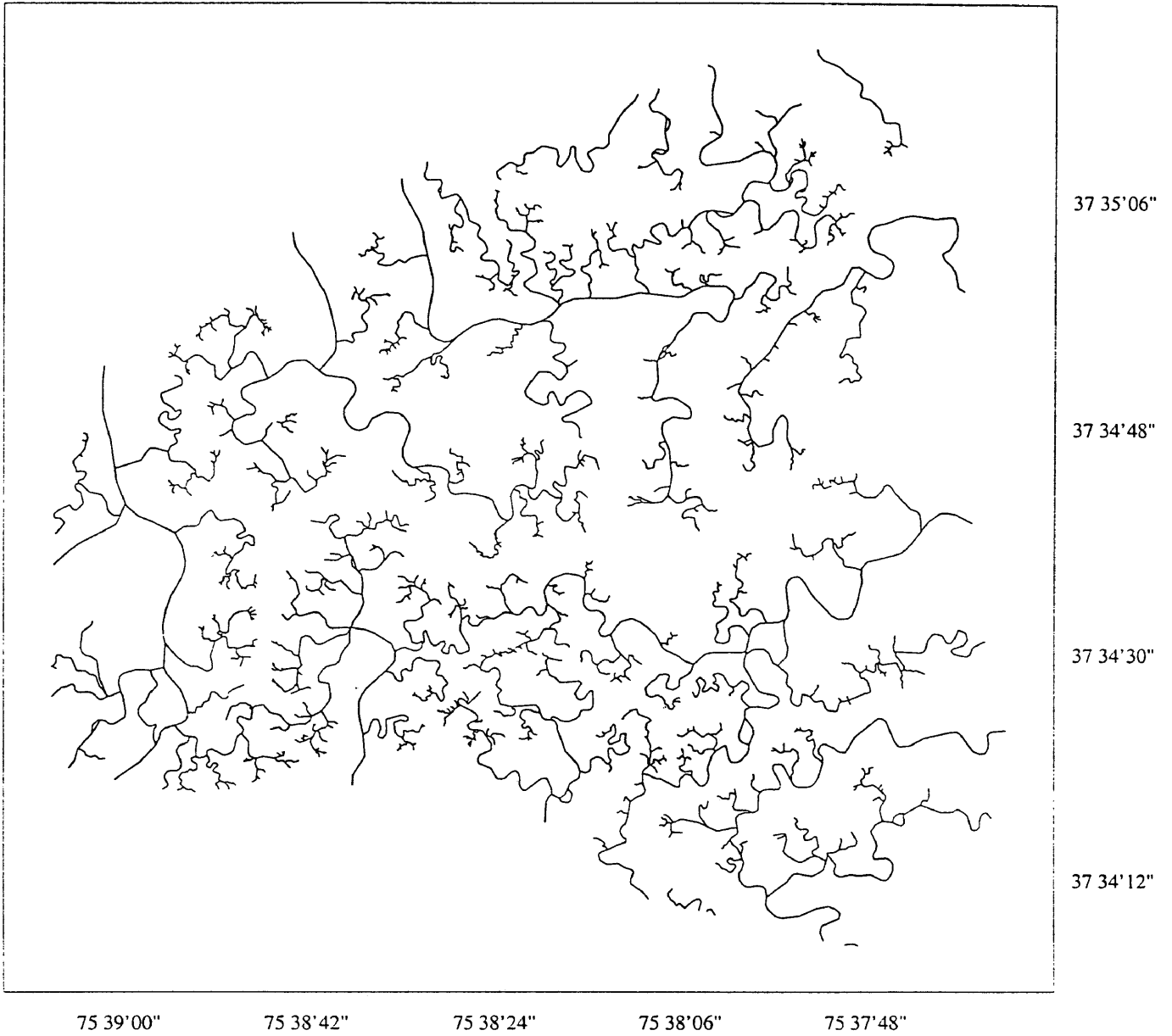


Figure 16

Wachapreague Marsh Drainage Network



that an appropriate range of mesh sizes for comparison of these three marshes is from 5 to 200 meters. Smaller mesh sizes provided no further information. The slope of the Richardson plot for smaller sizes is very close to -1, (between -1.01 and -1.00). Mesh sizes above 200 meters produce erratic results as the total number of boxes in the grid becomes small (12 boxes per side for the Wachapreague marsh). Mesh sizes were incremented logarithmically to equalize the sensitivity of the regressions to individual data points at both ends of the Richardson plot.

The Value Attribute Table produced by ARC-INFO for each grid was output to an ascii file. This file was input to a SAS program which calculated the number of boxes which contained an element of the creek network pattern for each box size.

Calculations of the slopes of the Richardson curves were also performed in SAS. Straight line regressions of consecutive five point moving subsets of the mesh sizes were used to estimate the tangent of each curve at the midpoint of the subset.

The traditional method of procuring the fractal dimension with the box-counting method is to use the estimated slope of a straight line regression through an arbitrarily chosen range of points of the Richardson plot, or often, when there are few points, to use all of them. The fractal dimension is simply the negative of the slope. Visual examination of the Richardson plots for the three marshes suggests that there are two fractal behaviors being expressed. Consequently, the Richardson plots were split into two ranges, and straight line regressions performed on the two subsets of points. In order to introduce some objectivity into choosing the slopes for multifractal behavior, the split point was determined by choosing the point which produced the greatest difference in slopes between the two lines.

Link analysis

The patterns of linkage points for each network was constructed in ARC-INFO. Pseudo-nodes, those nodes which do not occur at intersections of lines, were removed. The remaining nodes were then converted to a point coverage. This point coverage was then subjected to the same box-counting algorithm as the arc coverage was for the channel analysis.

Rotation and Origin Variation

ARC-INFO uses the upper right hand corner of the coverage as the origin for the arc to grid procedure, thus a rotation of coordinates around the center of the coverage results in a change of origin as well as a rotation of the overlaying grid used in the box-counting method. The creek network for the Wachapreague marsh was rotated about the center of the network at angles of 18, 36, 54, and 72 degrees. This was accomplished by transforming the tics of each coverage :

$$x' = (x - x_{shift}) * \cos\alpha - (y - y_{shift}) * \sin\alpha$$

$$y' = (x - x_{shift}) * \sin\alpha + (y - y_{shift}) * \cos\alpha$$

where x' , y' are the transformed coordinates, x_{shift} , y_{shift} determine the center point of rotation, and α is the degree of rotation desired. The arc coverage was then reprojected onto the transformed tic points, and subjected to the same box-counting algorithm.

Hyperbola Fitting of Richardson Plot

If the functional box-counting method is employed with a complete ideal range of box sizes, then the slope of the Richardson plot at the smallest box sizes must be equal to that of the lowest dimension of the element of the pattern being analyzed. For the channel analysis, the element of the pattern is linear, thus the slope at the smallest box sizes is -1. For the link analysis, the elements of the pattern are points, and the slope at the smallest box sizes is (-) 0. At large box sizes, every box contains an element of the pattern, and an increase in box size results in a concomitant decrease of the number of boxes counted by the square root of the increase. Thus, the slope at large box sizes is -2. The curve of Richardson plots may then be characterized by a hyperbola which has as its asymptotes a line with slope of zero for the link analysis, or negative one for the channel analysis, and a line with slope of negative two.

The Nelder-Meade simplex search method in Matlab was used to minimize the root mean square difference of the predicted hyperbola vs. the observed values of the log cell size and log cell count coordinates for each Richardson plot. The asymptotes for the channel analysis are:

$$y - y_0 = -(x - x_0)$$

$$y - y_0 = -2 * (x - x_0)$$

and the hyperbola to be fitted:

$$[(y - y_0) + (x - x_0)][(y - y_0) + 2 * (x - x_0)] = c$$

$$RMS = \frac{\sum (y - (y_0 + 1.5 * x_0 - 1.5 * x - (c + .25 * (x - x_0)^2)^{0.5})^2)}{(50 - 3)}$$

resulting in the function to be minimized:

$$RMS = \frac{\sum (y - (y_0 + 1.5 * x_0 - 1.5 * x - (c + .25 * (x - x_0)^2)^{0.5})^2)}{(50 - 3)}$$

where the parameters to be estimated are the center of the hyperbola at x_0 , y_0 , and the distance to the foci, c .

The asymptotes for the link analysis are:

$$y - y_0 = 0$$

$$y - y_0 = -2 * (x - x_0)$$

and the hyperbola to be fitted:

$$(y - y_0)[(y - y_0) + 2 * (x - x_0)] = c$$

and its corresponding function to be minimized:

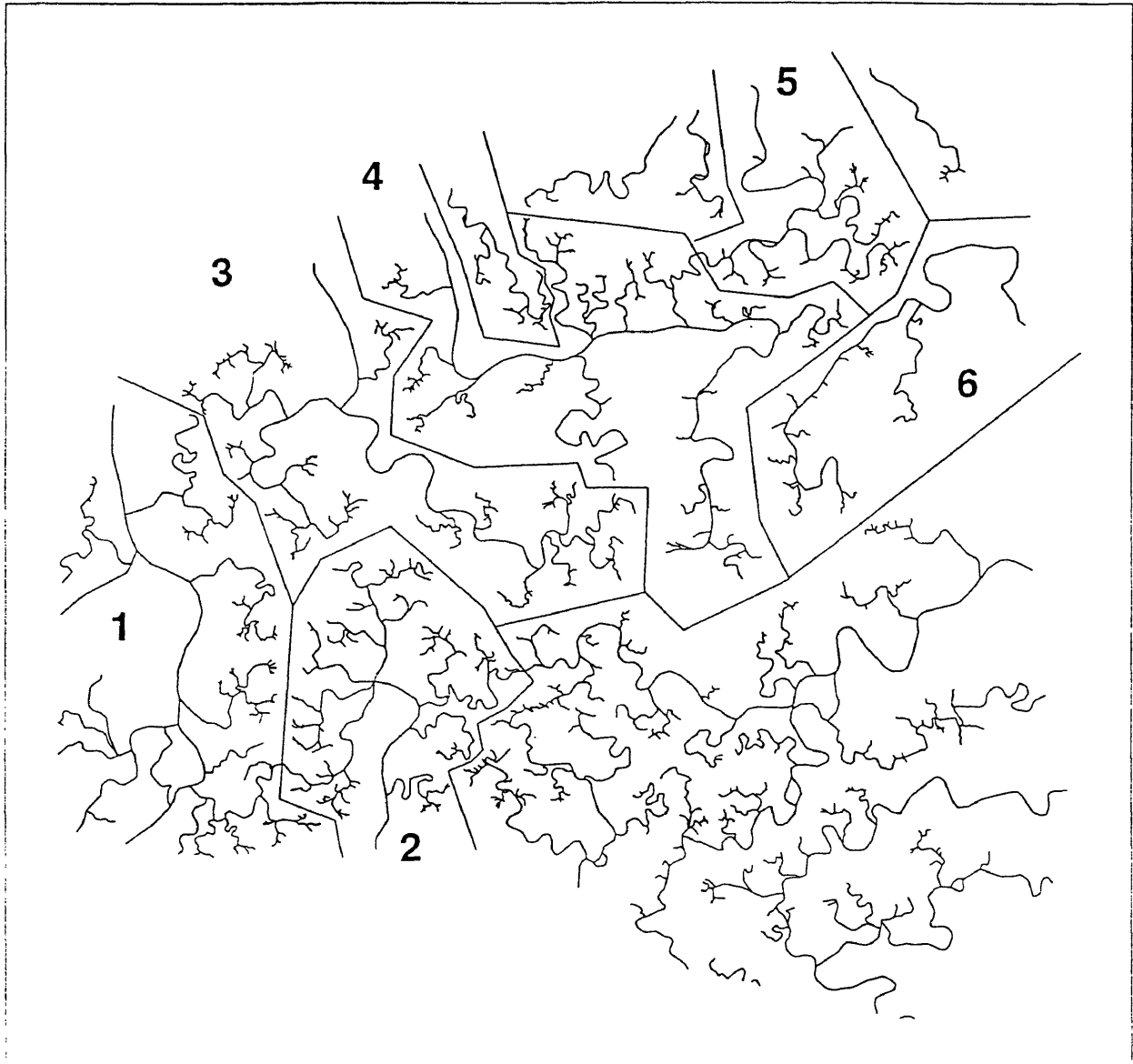
$$RMS = \frac{\sum (y - (y_0 - (x - x_0) - ((x - x_0)^2 + c)^{0.5})^2)}{(50 - 3)}$$

Hortonian Analysis

Of the three marsh systems, only the Wachapreague marsh system appeared to be amenable to Hortonian analysis. The drainage pattern of the marsh at Wachapreague allowed identification of several discrete drainage patterns which either were not connected to other patterns in the marsh, or connected minimally (Figure 17). A few islands were eliminated and 3 shallow creeks were separated in order to perform stream ordering on the discrete patterns. These separations occurred in shallow areas, usually in mudflats, and seemed to be natural boundaries between the 'watersheds'. Several of the resulting subpatterns were dendritic with little braiding. Six of these watersheds were chosen for Hortonian analysis. Streams were ordered according to the Strahler technique and bifurcation and length ratios were calculated for each watershed and overall (Tables 4,5). These values were used to calculate the fractal dimension using the derivation of La Barbera and Rosso (1987,1989, see Background section).

Figure 17

Watershed Divisions of Wachapreague Marsh Network



RESULTS

Channel Analysis

The Richardson plots for the three marshes are presented in Figure 18. Each curve consists of 50 mesh sizes in log increments from 5 to 200 meters. The Richardson plots look as would be expected from a fractal pattern. Note the bend in the middle of the plot, which occurs around box sizes of 55 meters. The intercept shifts are caused by the differences in total area of the networks. The slopes of all three marshes appear remarkably similar, and it is difficult to discern much difference between them.

The slopes of the lines can be more closely compared by plotting estimates of the tangents to the curve of the three marshes (Figure 19). As expected, the slopes start at close to negative one at small mesh sizes, and steepen at larger mesh sizes. Note that the magnitude of the slopes for Mockhorn Island are consistently less than those for the other two marshes, which appear to be equal. Compare these slopes with those obtained from an arbitrary nonfractal pattern in Figure 20. The non-fractal pattern has a constant slope of -1 for the smaller box sizes. Once the box size reaches a threshold value, that size where every box contains an element of the pattern, the slope jumps toward -2. In contrast, the slopes of the marsh drainage patterns change gradually from -1 to -2, expressing fractal behaviour between these extremes. In this range, the total measured length of the network drainage

Figure 18. Richardson Plots for Channel Analysis

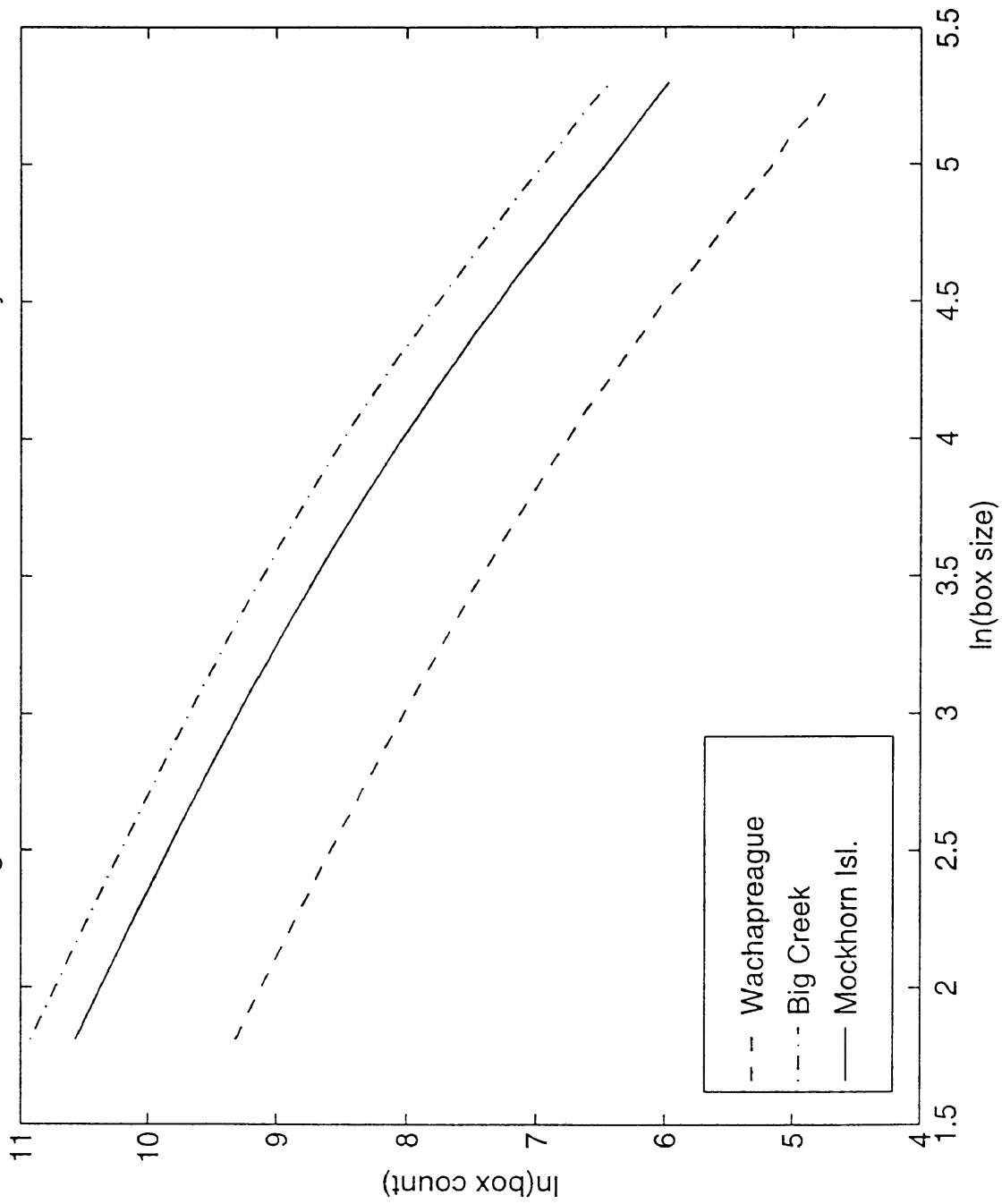


Figure 19. Tangents to Richardson Plots from Channel Analyses

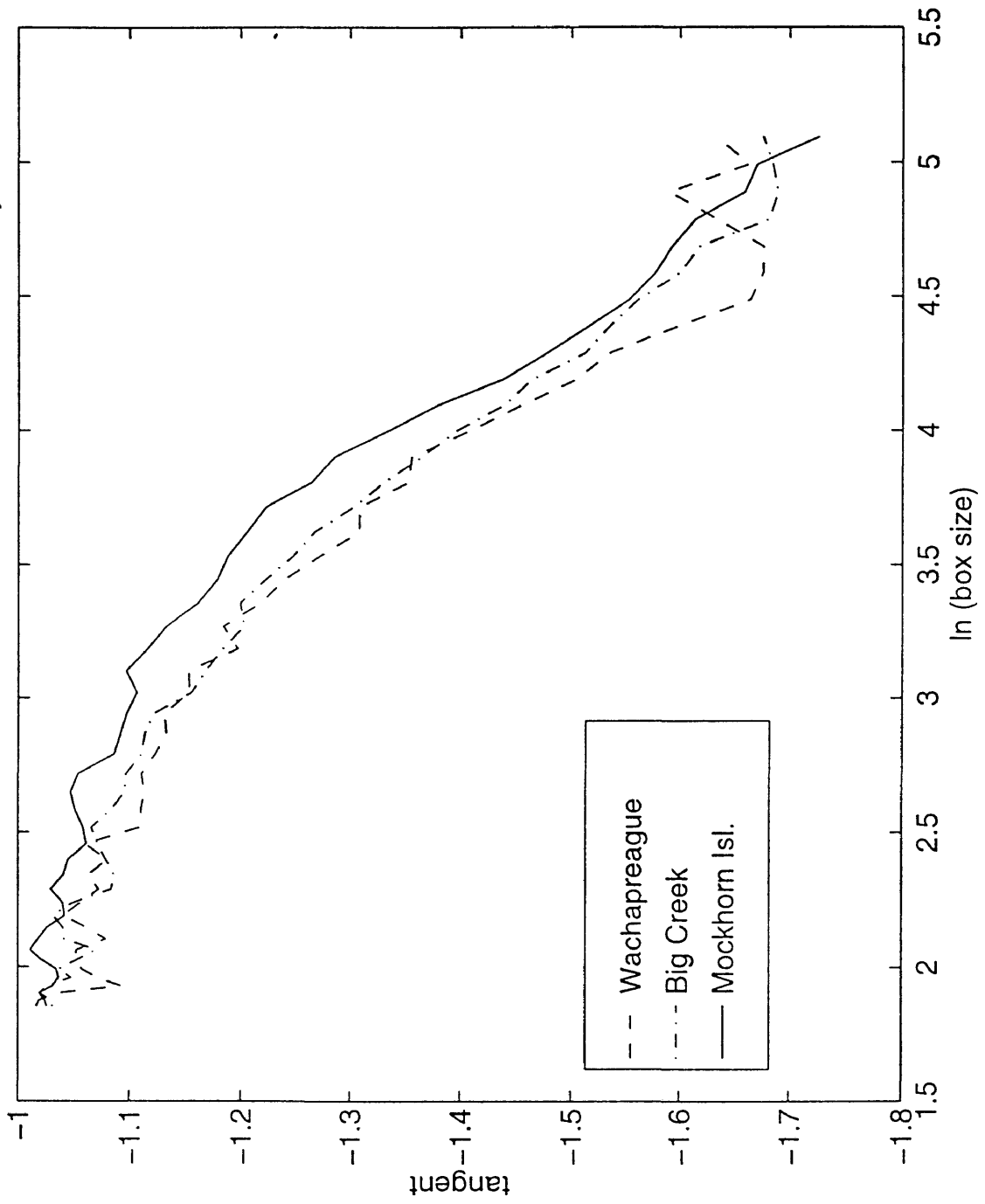
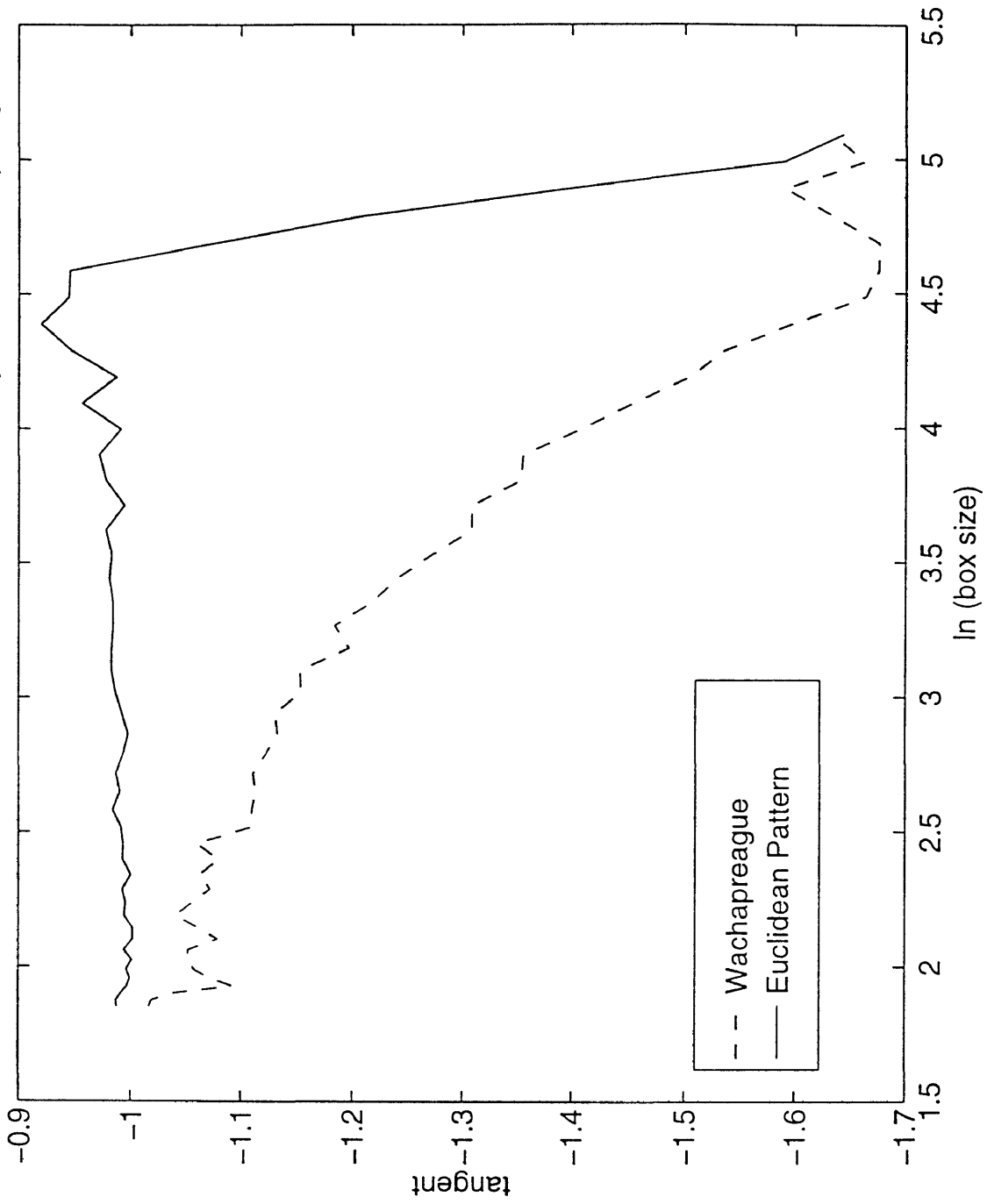


Figure 20. Tangents to Richardson Plots from Euclidean Analysis and Wachapreague Network



pattern is scale dependent. More precisely, the behaviour agrees with the definition of a physical fractal object according to Vicsek (1992), "In general, we *call a physical object fractal, if measuring its volume, surface or length with d , $d-1$ etc. dimensional hyperballs it is not possible to obtain a well converging finite measure for these quantities when changing l over several orders of magnitude*". The boxes in this case are analogous to 2 dimensional hyperballs, or sometimes called 2 dimensional cubes, for generalization of higher dimensional box-counting.

The fractal dimensions obtained from splitting the Richardson plots into two curves are presented in Table 1. Note again that the values for all three marshes are very similar. The Richardson Plot of Mockhorn Island does not have a maximum difference in slopes in the middle of the plot, but rather results in a constant increase of slope differences as the splitting threshold increases up to the largest mesh sizes. At a split of mesh size equal to 121 meters, the two slopes are -1.17 and -1.72. The regression for the mesh sizes greater than 121 meters is performed on only the 5 largest mesh sizes.

Link Analysis

Removing the linear elements from the drainage network patterns produces a pattern of points located at each of the creek intersections, called links, of the original network. If the branching pattern is fractal, then the distribution of the locations of the links should also be fractal, and the pattern of points is amenable to the functional box-counting technique. Extraction of the linear elements from the drainage pattern divests the pattern of the sinuosity characteristics, but preserves the fractal nature of the branching. The pattern of points thus

Table 1. Fractal Dimensions from Richardson Plots, Channel Analysis

<u>Marsh</u>	<u>split pt. (m)</u>	<u>small scale f.d.</u>	<u>large scale f.d.</u>
Wachapreague	55	1.14	1.63
Big Creek	90	1.18	1.68
Mockhorn Isl.*	121	1.17	1.72

* The large scale f.d. was determined from only the 5 largest mesh sizes, see text

produced for Wachapreague marsh is shown in Figure 21 and the Richardson plots for all three marshes for this link analysis is shown in Figure 22. The corresponding plots of the slopes of the tangents to these curves are calculated the same as for the channel analysis and shown in Figure 23. Note again the similarity of the three curves in the link analysis. At the smaller mesh sizes the slope of the curve is near zero, the dimension of the elemental points, and again, at around a mesh size of 55 meters the slope begins to steepen quickly.

Hyperbola Fitting of Richardson Plot

The results of fitting the Richardson curves to hyperbolas for each marsh and each analysis (channel and link) are shown in Table 2. The Nelder-Meade simplex search method was used to minimize the root mean square difference of the predicted vs. the observed values. Note from Figure 24 that the estimated hyperbolas fit the data very closely, suggesting that this estimation may be preferable to the traditional straight line fit of the Richardson plots.

Rotation and Origin Variation

Functional box-counting analysis was performed on the Wachapreague marsh system with the overlaying grids rotated about the center 18, 36, 54, and 72 degrees. Since the origin of the GRID subprogram of ARC-INFO uses the upper right corner as the origin, these rotations also resulted in a change of origin. The variations between the Richardson plots for

Figure 21

Wachapreague Marsh Linkage Pattern

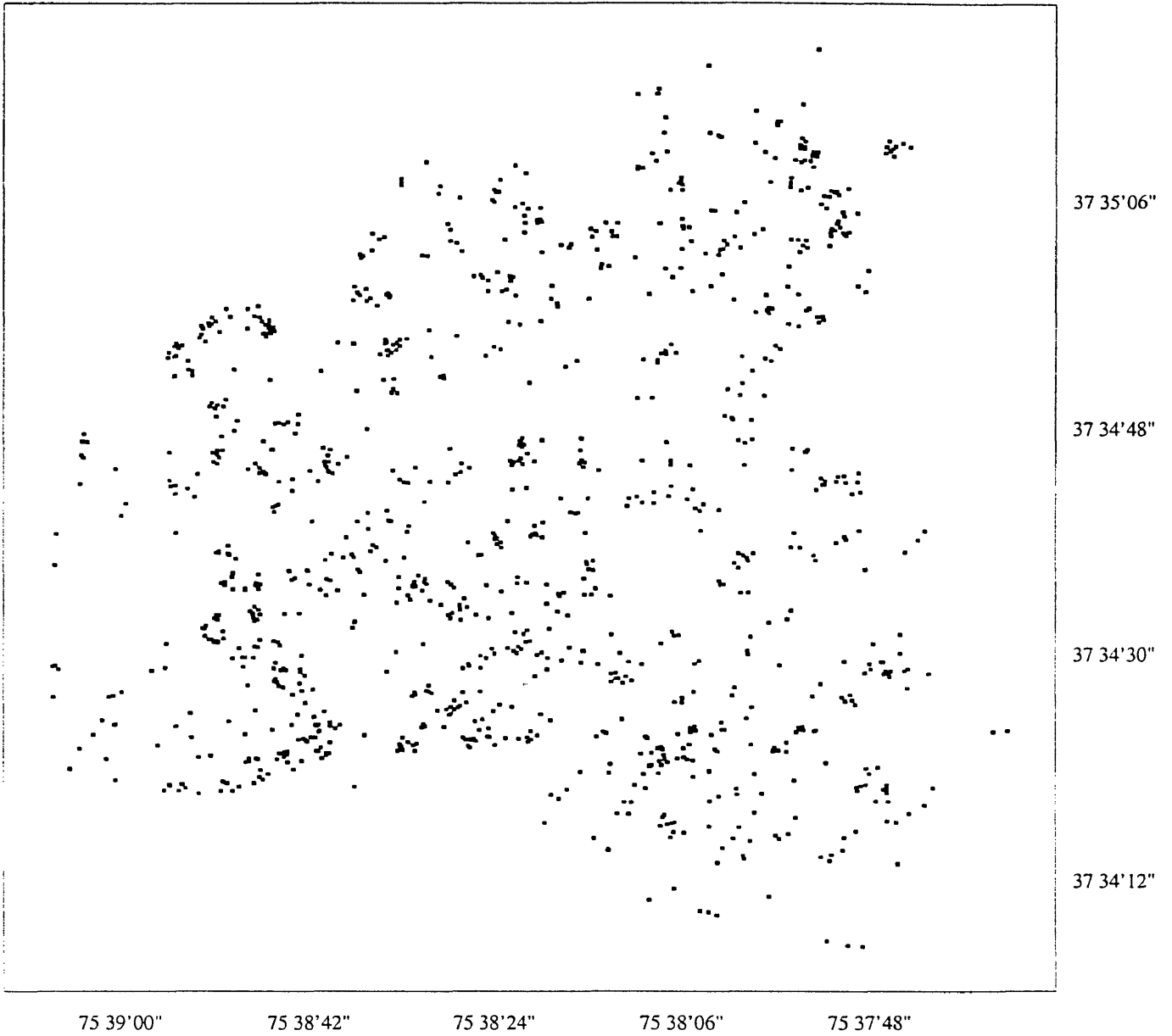


Figure 22. Richardson Plots from Link Analysis

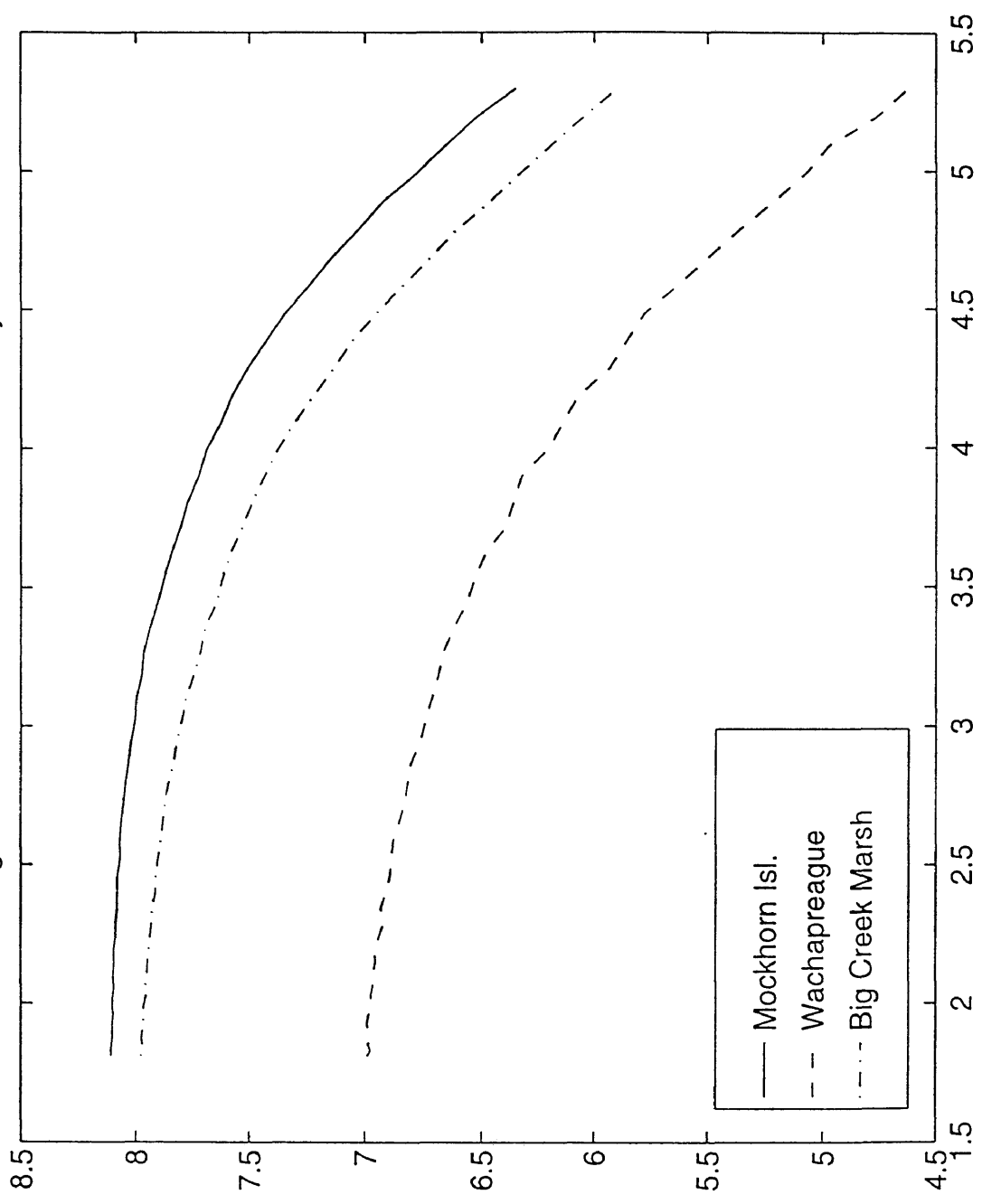


Figure 23. Tangents to Richardson Plots from Link Analyses

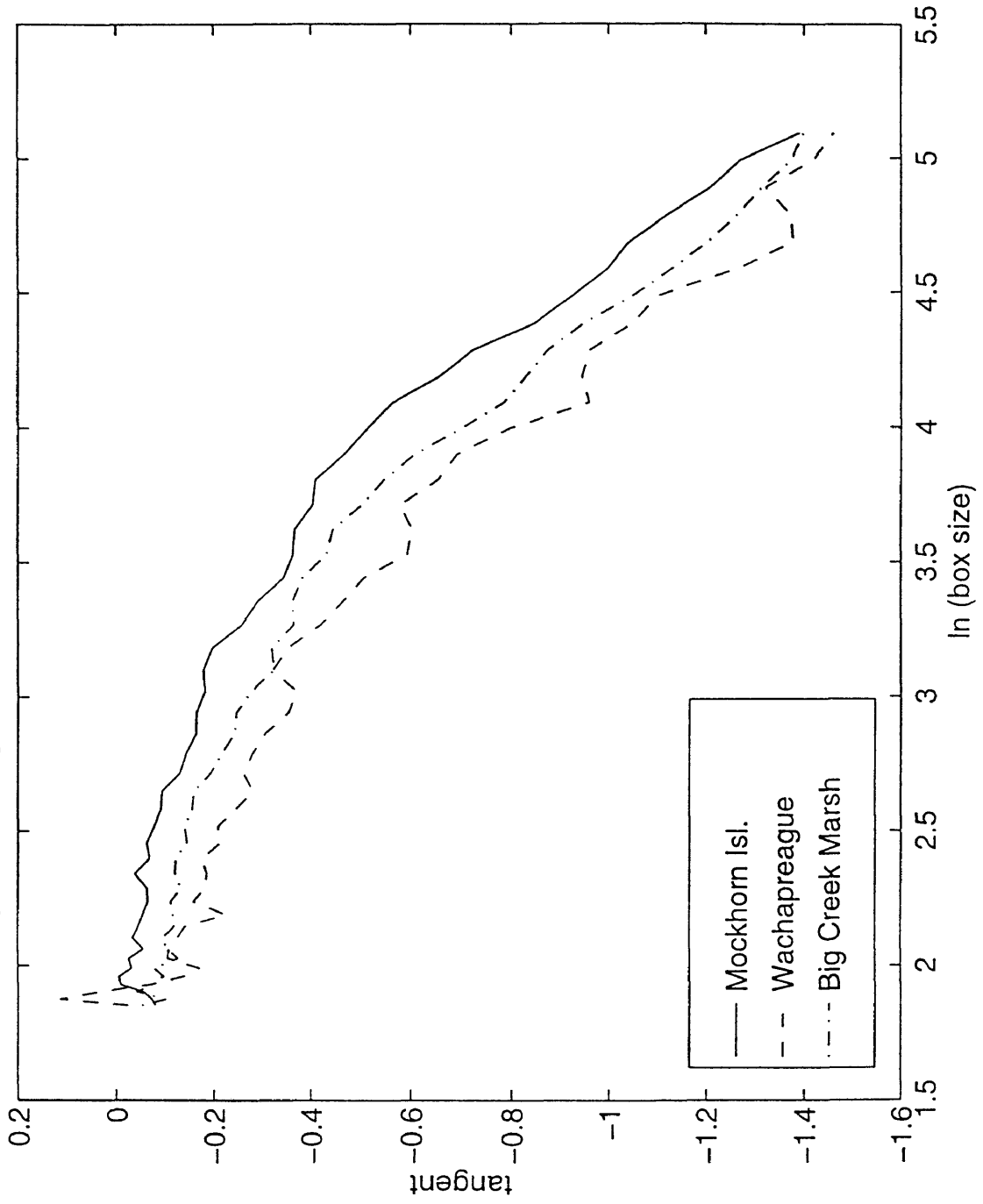


Table 2. Hyperbola Parameter Estimates

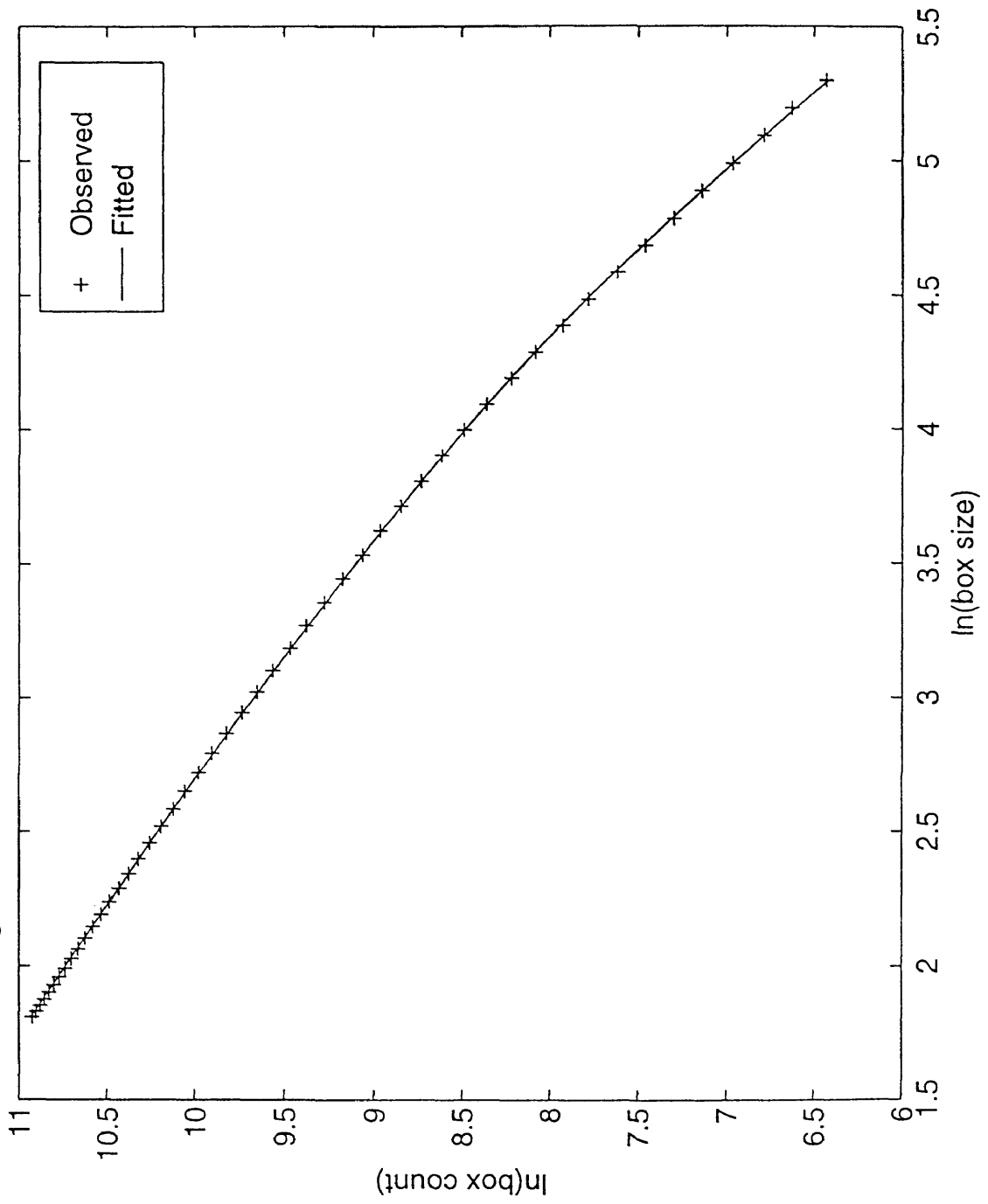
Channel Analysis

<u>Marsh</u>	<u>X</u> ₀	<u>Y</u> ₀	<u>C</u>
Wachapreague	4.26	7.03	0.430
Big Creek	4.32	8.22	0.408
Mockhorn	4.42	8.42	0.282

Link Analysis

<u>Marsh</u>	<u>X</u> ₀	<u>Y</u> ₀	<u>C</u>
Wachapreague	4.23	7.37	1.969
Big Creek	4.44	8.28	1.623
Mockhorn	4.60	8.33	1.185

Figure 24. Mockhorn Isl., Fitted and Observed Richardson Plot



these rotations, and the original georeferenced image, are so slight that the graphs lie on top of each other, so are not presented here. Table 3 presents the parameter estimates of hyperbola fitting the Richardson plots of the rotations. Note the close similarity of the estimates and the low root mean square errors. It appears that for marsh drainage networks, a single grid orientation and origin provides a robust estimate of the network's fractal behaviour.

Hortonian Analysis

La Barbara and Rosso (1989) as well as others (see Background) derived fractal dimensions from the bifurcation and stream length ratios of dendritic river drainage systems. The derivations depend upon the Hortonian assumptions of constant bifurcation and length ratios over all stream orders. Whether this assumption holds true for the ratios by watershed or over all watersheds is problematic. Examination of the results across watersheds in Table 5 suggests that the stream length ratios seem to be fairly constant, but the bifurcation ratios appear have two modes, about 1.9 for stream orders 1 through 3, and about 3.2 for stream orders 3 through 5. Using Tarboten et al's (1989) equation results in a fractal dimension of 2.2 including all orders of streams, while using just orders 1 through 3 results in $D = 1.3$.

Table 3. Hyperbola Parameter Estimates for Rotations of Wachapreague Marsh

<u>Rotation (degrees)</u>	<u>X₀</u>	<u>Y₀</u>	<u>C</u>	<u>RMS Error</u>
0	4.26	7.03	0.430	.00015
18	4.22	7.07	0.406	.00015
36	4.23	7.07	0.411	.00009
54	4.25	7.04	0.410	.00020
72	4.23	7.04	0.410	.00005

Table 4. Hortonian Analysis of Wachapreague Marsh by Watershed

Across watersheds:

<u>Watershed</u>	<u>Order</u>	R_b	R_l
1	1	1.69	1.88
	2	2.60	5.48
	3	5.0	4.58
	4	0.75	1.53
2	1	1.87	2.97
	2	1.73	3.90
	3	11.0	11.89
	4	0.67	0.81
3	1	1.55	2.20
	2	3.0	6.65
	3	2.43	5.62
	4	3.5	3.75
4	1	1.88	2.68
	2	1.88	3.46
	3	1.54	1.47
5	1	2.06	3.47
	2	1.50	2.37
	3	2.40	4.48
6	1	3.00	4.03
	2	0.60	0.97

Table 5: Hortonian Analysis of Wachapreague Marsh

Across watersheds:

<u>Order</u>	R_b	R_l
1	1.799	1.355
2	1.978	2.079
3	3.321	1.325
4	3.111	1.340
mean	2.552	1.525

All orders:

$$D = (\ln(R_b)) / (\ln(R_l)) = .937/.422 = 2.22$$

Orders 1-2:

mean	1.88	1.6
------	------	-----

$$D = .63/.47 = 1.34$$

DISCUSSION

Box-counting Technique

Virtually all of the regressions performed in these results had R-square coefficients greater than .99. In fact, a regression of any arbitrarily chosen subset of points on the Richardson plot will produce an almost perfect R-square. Thus it is tempting to conclude confidently that the negative of the slope is the value of the fractal dimension.

Most estimates of the fractal dimension using the box-counting technique in the literature are performed on very few points. In this study, the automation of this technique with computer software has provided the opportunity to perform sampling at small intervals across a broad range of scales. Closer inspection of the tangents of the Richardson plot reveals a constant gradual change of the slope across the sampled range, and no obvious range over which there is a constant slope, except at the very small mesh sizes where the slope is essentially -1. This leads to the condition that for small samples of mesh sizes, the slope obtained is very dependent upon the choice of mesh sizes.

One explanation of the lack of a distinct constant slope over a specific range of mesh sizes is that it is the result of two overlapping self similar regions. The smaller mesh sizes reveal the degree of sinuosity of the channels, the linear elements of the creek network

pattern. At larger mesh sizes, the branching pattern begins to be revealed. If these ranges overlap, then we should get a gradual transition from one slope to the other. Similar results were found by Tarboten et al (1989) for a drainage networks derived from Digital Elevation Maps (DEM's).

Tarboten et al's results found slopes much closer to -2.0 at large mesh sizes than were found for marshes in this study. I believe this is partially an artifact of the derivation of the network from DEM's, instead of real streams. This slope at large mesh sizes, they argue, is evidence that the drainage basin is completely space filling, as would be intuited from the fact that the entire area must be drained. However, salt marsh drainage networks discharge significant amounts of water over the marsh and by lateral transport through sediment macropores (Yelverton and Hackney, 1986, Whiting and Childers, 1989, Harvey et al 1987). Marshes with less hydraulically conductive substrate matrices may necessarily have more space filling drainage networks, and therefore fractal dimensions closer to 2.

In addition to the probable multi-fractal nature of the pattern, a more fundamental characteristic of the Richardson plots is responsible for the nonlinearity of the curve. As discussed previously, the slope of the curve at the finest resolution of the pattern must be of the same dimension of the pattern. For the channel analysis, the one dimensional elements of the creeks mandate that at small resolutions the slope of the Richardson plot must be -1. For the link analyses, the 0 dimension of the points results in a slope of 0 at fine resolutions. The points of the link analysis and the lines representing the creeks are distributed across a flat area. Therefore, at large resolutions, when all of the pattern has been covered, the slope of the Richardson plot must be -2. Had the points and lines been distributed in 3-space, the slopes at large resolutions would be -3. The results of this study suggest that the way in

which the curve of the Richardson plot approaches its two asymptotes is more indicative of the fractal nature, than an estimated straight line slope over a specific range. Note again the comparison in Figure 20 of the fractal pattern and the Euclidean pattern. A random sparse sampling of box sizes of the Euclidean pattern may well have resulted in the same straight line slope as that of the fractal marsh pattern.

The characterization of the Richardson plot as a hyperbola may sufficiently describe the multifractal behavior of a specific pattern, allowing quantitative comparisons of different patterns, and obviating the arbitrary selection of ranges on the Richardson plot used to determine a specific value for one or more fractal dimensions.

Relationship between Link and Channel Analysis

Figure 25 compares the slopes from the link analysis with those of the channel analysis. For any given mesh size, the link analysis always has a shallower slope than that of the channel analysis. This reflects the inability of the channel analysis to distinguish between the linear effects of the drainage pattern and the branching effects, at larger mesh sizes.

It is important to remember that the fractal dimension of the channel and link analyses describe different attributes. The channel analyses describe how the total measured length of the network changes with a change in the scale, while the link analyses describe how the observed number of intersections of the network changes with a change of scale. Clearly, as more and more intersections are resolved in the network at smaller scales, the total measured length of the network must also increase. But the link analysis does not indicate how quickly

the total measured length changes with changing scale, and could not, as there is no information about the sinuosity of the channels in the point pattern of link locations. Therefore, while the self similar branching behavior may be dominant at the larger mesh sizes in the channel analysis, it should not be expected to have the same fractal dimension as that expressed in the link analysis, even at the same larger mesh sizes.

The relationship between the two fractal behaviors may be more closely examined by plotting the slopes of the respective Richardson plots for each mesh size (Figures 26-28). Note that for all marshes at small mesh sizes there seems to be little relation between the two (plot goes from large mesh sizes in the lower left to small mesh sizes in the upper right). In the midscale mesh sizes, especially for Mockhorn Island, and to some degree in Big Creek marsh, the departure of the graph from a slope of 2 indicates that the rate of change of slope is different for the two fractal behaviors in this range. As the plot goes from smaller mesh sizes to larger mesh sizes, the slope of the channel analyses changes more quickly than the change of slope of the link analyses. This suggests that within this range of scales that the change in total measured length (channel analysis) is more of a result from the sinuosity of the creeks than from the degree of branching. Eventually, both slopes must reach -2, and this is reflected in the return of the curve to the slope -2 .

Hypothesis Testing of Richardson Plots

One of the underlying assumptions for testing of difference of slopes of two or more different regressions is that the dependent values ($\ln(\text{number of boxes counted})$) are independent and identically distributed for each 'x' value ($\ln(\text{box size})$). This is not the case

Figure 25. Tangents to Richardson Plots from Channel and Link Analyses, Mockhorn

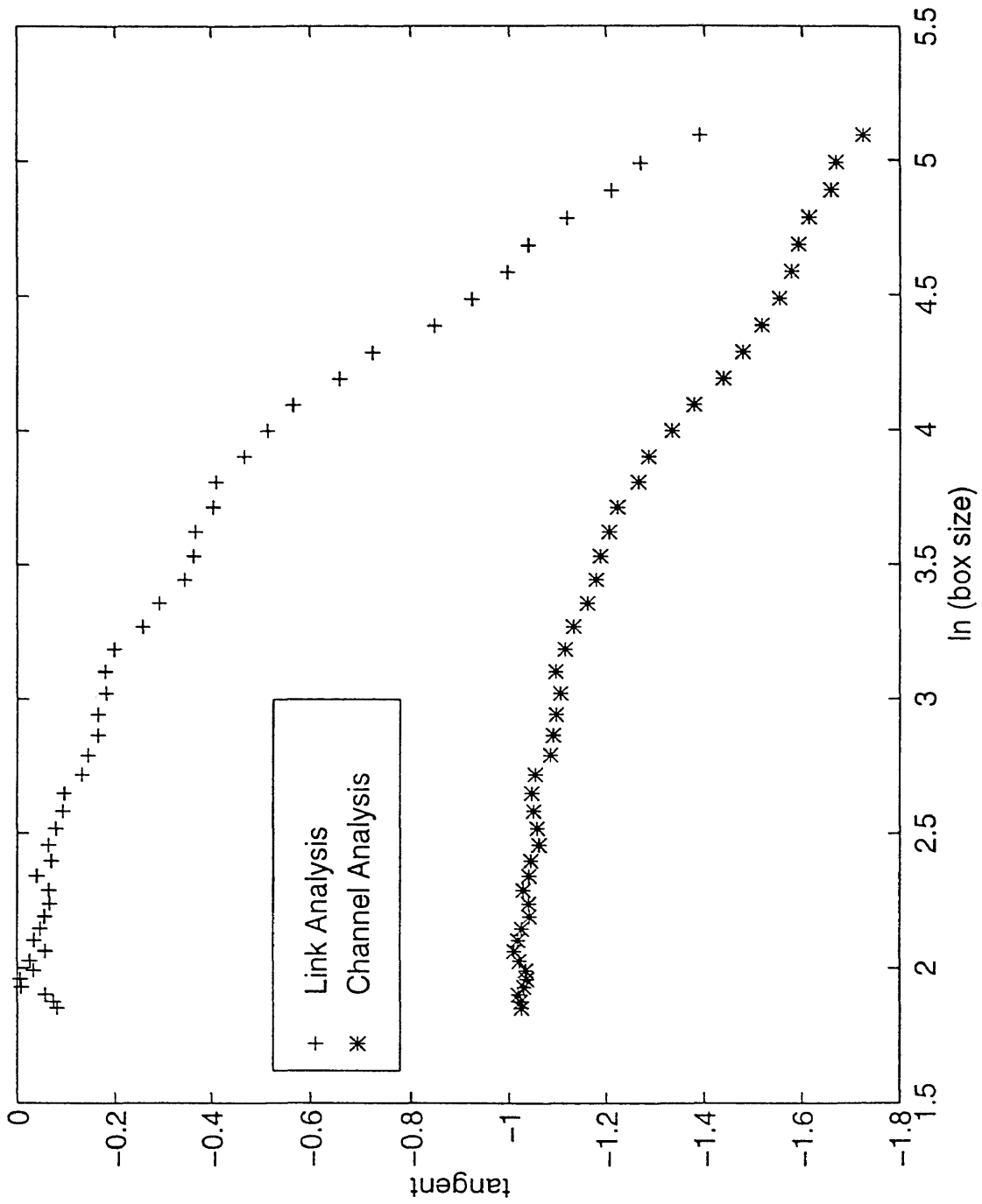


Figure 26. Tangents, Link vs. Channel Analysis, Mockhorn

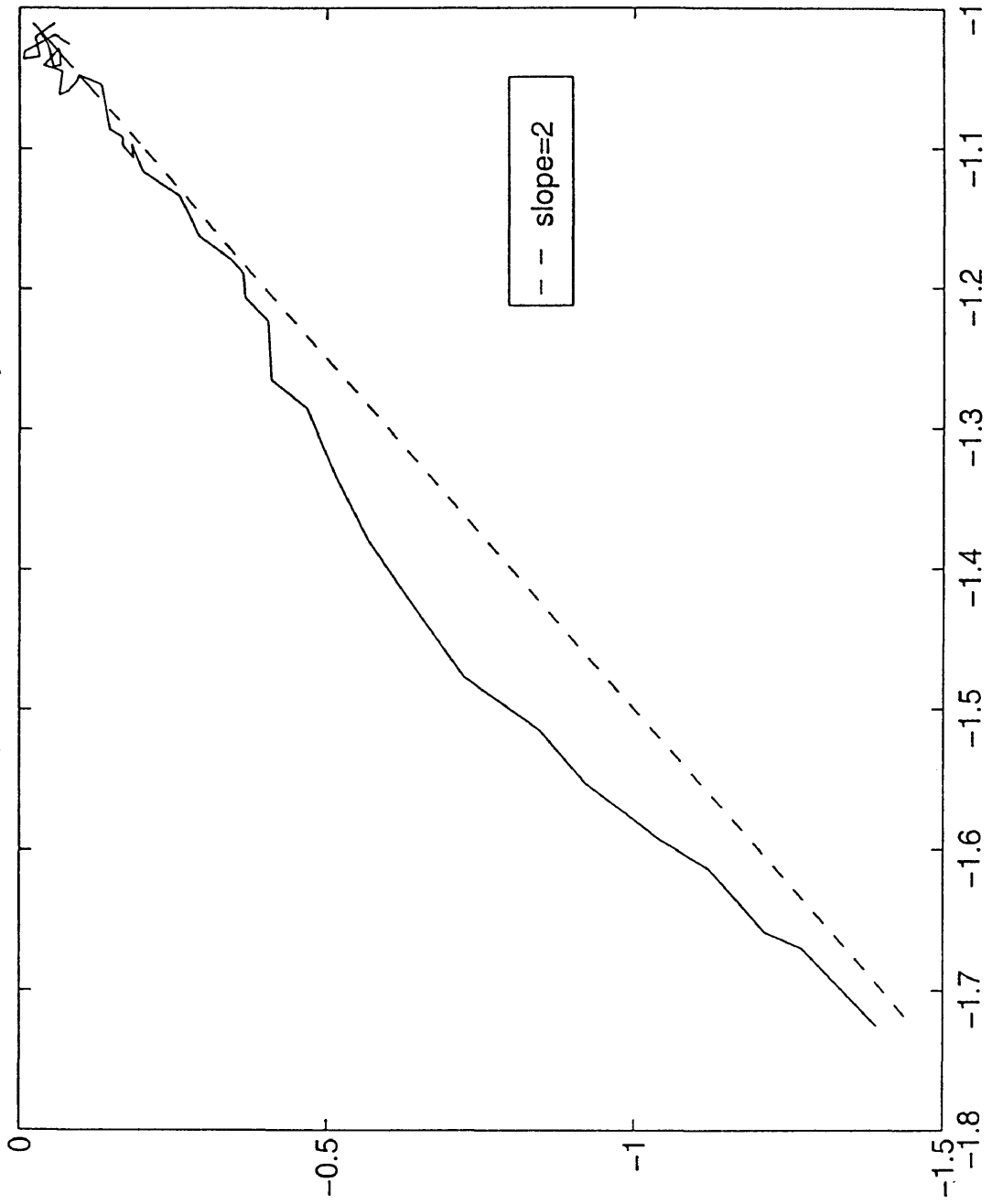


Figure 27. Tangents, Link vs. Channel Analysis, Big Creek

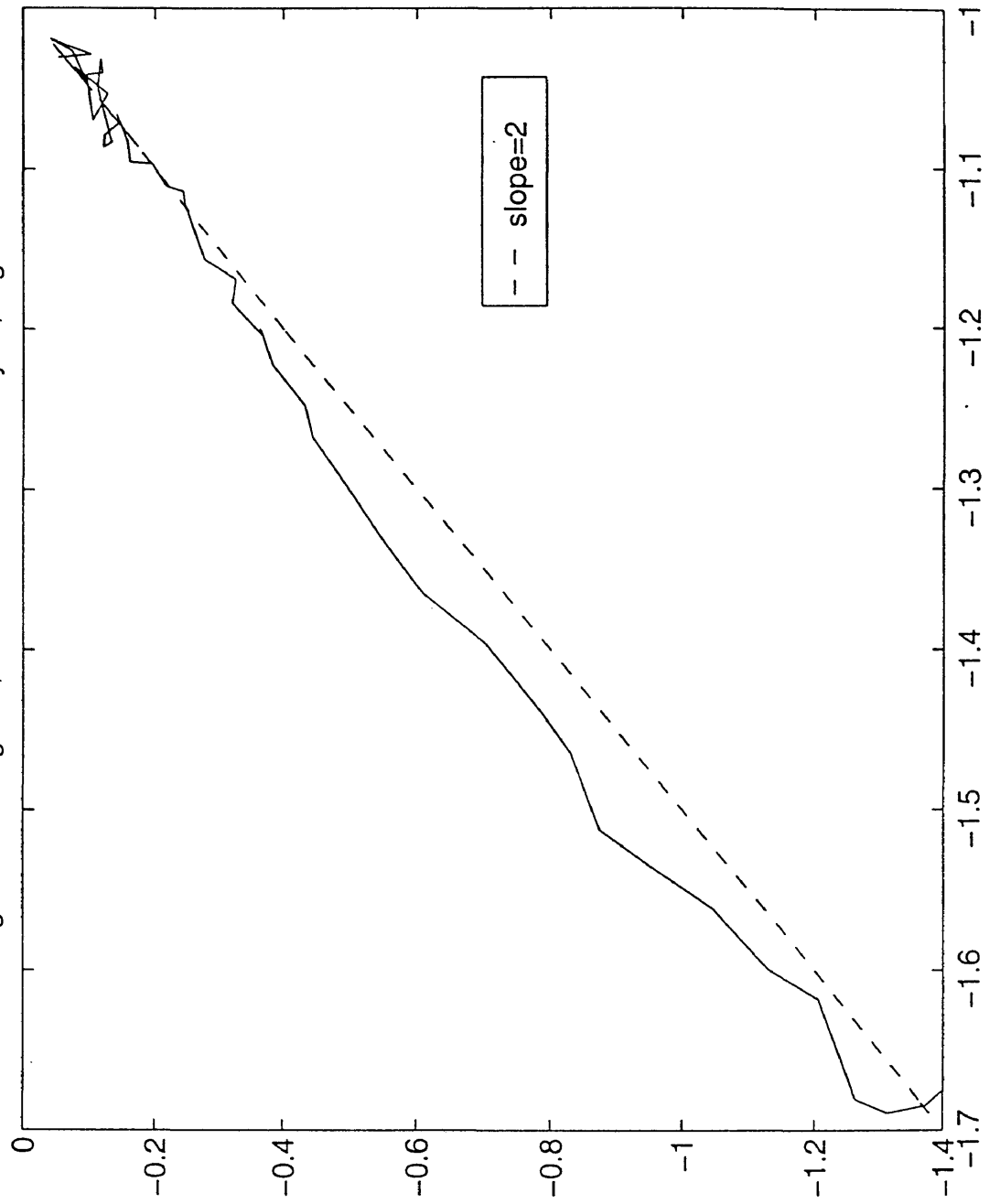
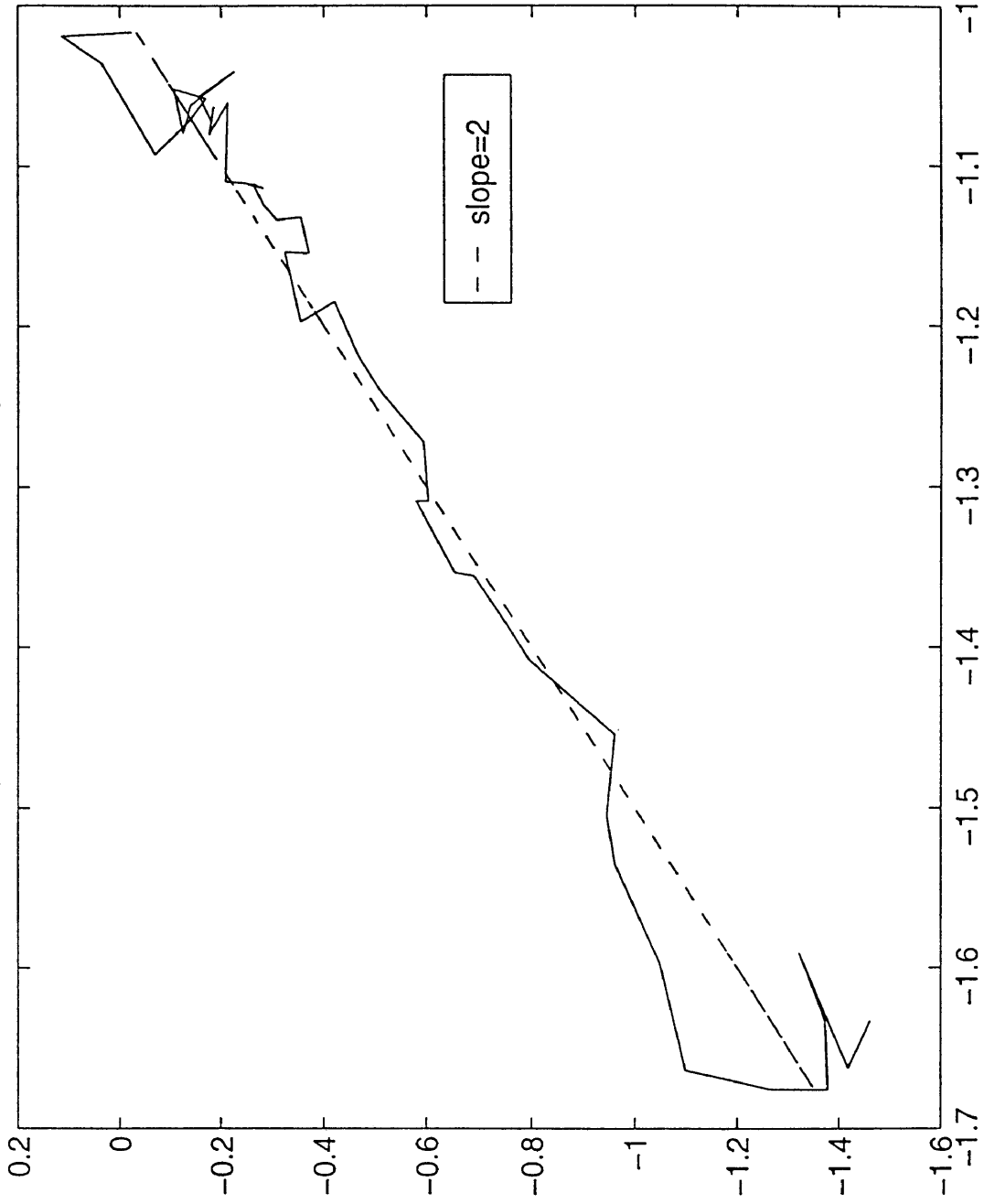


Figure 28. Tangents, Link vs. Channel Analysis, Wachapreague



for the points in a Richardson plot. Once a grid origin and orientation are established, the $\ln(\text{number of boxes counted})$ is determined for each and every value of box-size chosen, that is to say, they are not independent. The same holds true for the parameter estimates of the hyperbolic curves. The residual errors for the estimated slopes of the Richardson plots are intentionally not reported here to prevent their misuse for testing for differences in slopes.

It may be possible to consider the entire pattern under investigation as a population where the population statistic to be estimated is the fractal dimension. Each grid origin/orientation is a sample point, from which an estimated fractal dimension is derived. By random sampling of grid origin/orientation values, an estimate of population parameter and population variance of the parameter may be obtained. The investigation of the robustness of choice of origin/orientation essentially employs a systematic random sampling method. The original orientation is a random grid origin/orientation value, and subsequent samples are systematically rotated 18 degrees. If this type of sampling was performed upon the other two marsh patterns, it may be possible to jointly test for equality of the three parameter x_0 , y_0 , and c . Inspection of Table 3 suggests that if the other two marshes had a similar variance of the parameters, that the estimated value for the c parameter of Mockhorn Island would be significantly different from the other two marshes. The difference is also suggested by the plots of slopes in Figures 19 and 23.

CONCLUSIONS

Based on the comparison of the Richardson plots for the marsh drainage systems and a non-fractal pattern, the drainage network patterns of the three marshes are indeed fractal, and the fractal behavior of all three marshes are remarkably similar. This supports the idea that marsh drainage patterns from marshes with similar evolution, hydrology, and underlying geology should display similar fractal behavior. Because of the gradually changing slope of the Richardson plots of the three marshes it is difficult to ascertain an exact value or values of the fractal dimensions. The comparison of the channel analyses and the link analyses indicate that there are at least two types of fractal behavior in the patterns, namely, sinuosity and branching. The parameters estimated from fitting the Richardson plots to a hyperbola provide an alternative quantitative way of measuring the fractal behavior of a pattern. The box-counting technique is extremely robust with respect to the choice of origin and rotation of the overlaying grids. In the one marsh in which it was possible to identify discrete drainage patterns, Horton's assumptions of constant bifurcation and length ratios did not appear to be supported, and use of the theoretically derived fractal dimension from these values is suspect.

IMPLICATIONS

The establishment of the fractal nature of tidal creek drainage networks allows further research into the development of their patterns. Similar fractal behavior has been demonstrated for marshes with similar tidal range and evolution. Now it is possible to quantitatively compare these marshes with marshes of different environments and history. We may be able to ascertain the evolutionary history or the ecological role of specific marshes simply by measuring the fractal dimension of the drainage network pattern.

Methods to determine the fractal dimension of patterns other than the box-counting technique warrant investigation.

A numerical model of marsh creek evolution may be developed from the laws of minimum energy expenditure and field measurements of factors which determine the energy expenditure of water flow in a creek. These factors include the slope and hydraulic radius of the creeks, the tidal regime, the discharge, and the critical shear stress of the bed. By comparing the fractal dimension of the model output with those of actual marsh drainage patterns, it will be possible to elucidate the dominant factors which determine the patterns of tidal drainage creeks. This information will be invaluable for predicting changes which may be caused by anthropogenic or natural perturbations of an existing drainage system. Construction of functional, stable, drainage networks for wetland mitigation projects will also be aided by this information.

LITERATURE CITED

- Barnsley, M., *Fractals Everywhere*, Academic Press, Inc., Boston, 1988.
- Beer, T., and Borgas, M., Horton's Laws and the fractal nature of streams, *Water Resources Research*, 29(5):1475-1487; 1993.
- Boon, J.D. and Byrne, R.J., On Basin hypsometry and the morphodynamic response of coastal inlets, *Marine Geology*, 40:27-48; 1981.
- Escartin, J., and Aubrey, D.G., Flow Structure and Dispersion within Algal Mats, *Estuarine, Coastal and Shelf Science*, 40:451-472; 1995.
- Friedrichs, C.T. and Aubrey, D.G., Non-linear tidal distortions in shallow well-mixed estuaries: a synthesis, *Estuarine Coastal Shelf Science*, 27: 521-545; 1988.
- Frisch, A.A., Particle shape analysis based on the fractal dimension, dissertation; 1988.
- Garcia-Ruiz, J.M., and Otalora, F., Fractal trees and Horton's laws, *Mathematical Geology*, 24(1):61-71; 1992.
- Garofalo, D., The influence of wetland vegetation on tidal stream channel migration and morphology, *Estuaries*, 3(4): 258-270; 1980.
- Helmlinger, K.R., Kumar, P., and Foufoula-Georgiou E., On the use of digital elevation model data for Hortonian and fractal analyses of channel networks, *Water Resources Research*, 29(8): 2599-2613; 1993.
- Hjelmfelt, A.T. Jr., Fractals and the river-length catchment-area ratio, *Water Resources Research*, 24(2):455-459; 1988.
- Jordan, T.E., and Correll, D.E., Continuous automated sampling of tidal exchanges of nutrients by brackish marshes, *Estuarine, Coastal and Shelf Science*, 32:527-545; 1991.
- La Barbera, P., and Rosso, R., On the fractal dimension of stream networks, *Water Resources Research*, 25(4): 735-741; 1989.

- Leopold, L.B. and Langbein, The concept of entropy in landscape evolution, Geological Survey Profession Paper 500-A; 1962.
- Lovejoy, S., Schertzer, D., and Tsonis, A.A., Functional Box-counting and multiple elliptical dimensions in rain, *Science*, 235: 1036-1038; 1987.
- Marani, A., Rigon, R., and Rinaldo, A., A note on fractal channel networks, *Water Resources Research*, 27(12): 3041-3049; 1991.
- Mandelbrot, B.B, *The fractal geometry of nature*, W.H. Freeman, New York; 1982.
- Mitsch, J.M., and Gosselink, J.G., *Wetlands*, Van Nostrand Reinhold, New York; 1986.
- Nikora, V.I., Fractal structures of river plan forms, *Water Resources Research*, 27(6):1327-1333; 1991.
- Nikora, V.I., Sapozhnikov, V.B, and Noever, D.A., Fractal Geometry of individual river channels and its computer simulation, *Water Resources Research*, 29(10):3561-3568; 1993.
- Nikora, V.I., and Sapozhnikov, V.B, River network fractal geometry and its computer simulation, *Water Resources Research*, 29(10): 3569-3575; 1993.
- Oertel, G.F., Wong, G.T.F., Conway, J.D., Sediment accumulation at a fringe marsh during transgression, Oyster Virginia, *Estuaries*, 12(1):18-26; 1989.
- Osgood, D.T., Zieman, J.C., Spatial and temporal patterns of substrate physicochemical parameters in different-aged barrier island marshes, *Estuarine Coastal Shelf Science*, 37(4): 421-436; 1993.
- Per Bak, C.T., and Wiesenfeld, K., Self-organized criticality: An explanation of $1/f$ noise, *Physical Review Letters*, 59(4): 381-384; 1987.
- Pestrong, R., The development of drainage patterns on tidal marshes, *Stanford Univ. Pub.s*, 10(2); 1965.
- Rhea, S., Geomorphic observations of rivers in the Oregon Coast Range from a regional reconnaissance perspective, *Geomorphology*, 6: 135-150; 1993.
- Richardson, L.F., The problem of contiguity: An appendix of statistics of deadly quarrels, *General Systems Yearbook*, 6: 139-187; 1961.
- Robert, A., and Roy, A.G., On the fractal interpretation of the mainstream length-drainage area relationship, *Water Resources Research*, 26(5): 839-842; 1990.

- Rodriguez-Iturbe, I., et al, Fractal structures as least energy patterns: The case of river networks, *Geophysical Research Letters*, 19(9): 889-892; 1992.
- Rosso, R., Bacchi, B., and La Barbera, P., Fractal relation of mainstream length to catchment area in river networks, *Water Resources Research*, 27(3): 381-387; 1991.
- Snow, R.S., Fractal Sinuosity of stream channels, *Pure and Applied Geophysics*, 131(1/2):99-109; 1989.
- Stark, C.P., An invasion percolation model of drainage network evolution, *Nature*, 352:423-425; 1991.
- Stevens, P.S., *Patterns in Nature*, Atlantic-Little, Brown; 1974.
- Tarboton, D.G., Bras, R.L., and Rodriguez-Iturbe, Comment on "on the fractal dimension of stream networks", *Water Resources Research*, 26(9): 2243-2244; 1990.
- Tarboton, D.G., Bras, R.L., and Rodriguez-Iturbe, The fractal nature of river networks, *Water Resources Research*, 24(8): 1317-1322; 1988.
- Vicsek, T., *Fractal Growth Phenomena (Second Edition)*, World Scientific; 1992.
- Voss, R.F., Fractals in nature: From characterization to simulation, in *The Science of Fractal Images*, ed.s, Peitgen, H.O, and Saupe, D., Springer Verlag, New York; 1988.
- Wildish, D.J., and Miyares, M.P., Filtration rate of blue mussels as a function of flow velocity: Preliminary experiments, *Journal of Experimental Biology and Ecology*, 142(3): 213-219; 1990.